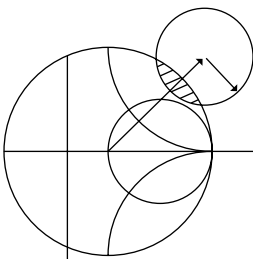


DAVID M. POZAR

MICROWAVE ENGINEERING

FOURTH EDITION



Transmission Lines and Waveguides

One of the early milestones in microwave engineering was the development of waveguide and other transmission lines for the low-loss transmission of power at high frequencies. Although Heaviside considered the possibility of propagation of electromagnetic waves inside a closed hollow tube in 1893, he rejected the idea because he believed that two conductors were necessary for the transfer of electromagnetic energy [1]. In 1897, Lord Rayleigh (John William Strutt) mathematically proved that wave propagation in waveguides was possible for both circular and rectangular cross sections [2]. Rayleigh also noted the infinite set of waveguide modes of the TE and TM type that were possible and the existence of a cutoff frequency, but no experimental verification was made at the time. The waveguide was then essentially forgotten until it was rediscovered independently in 1936 by two researchers [3]. After preliminary experiments in 1932, George C. Southworth of the AT&T Company in New York presented a paper on the waveguide in 1936. At the same meeting, W. L. Barrow of MIT presented a paper on the circular waveguide, with experimental confirmation of propagation.

Early RF and microwave systems relied on waveguides, two-wire lines, and coaxial lines for transmission. Waveguides have the advantage of high power-handling capability and low loss but are bulky and expensive, especially at low frequencies. Two-wire lines are inexpensive but lack shielding. Coaxial lines are shielded but are a difficult medium in which to fabricate complex microwave components. Planar transmission lines provide an alternative, in the form of stripline, microstrip lines, slotlines, coplanar waveguides, and several other types of related geometries. Such transmission lines are compact, low in cost, and capable of being easily integrated with active circuit devices, such as diodes and transistors, to form microwave integrated circuits. The first planar transmission line may have been a flat-strip coaxial line, similar to a stripline, used in a production power divider network in World War II [4], but planar lines did not see intensive development until the 1950s. Microstrip lines were developed at ITT laboratories [5] and were competitors of stripline. The first microstrip lines used a relatively thick dielectric substrate, which accentuated the non-TEM mode behavior and frequency dispersion of the line. This characteristic made it less desirable than stripline until the 1960s, when much thinner substrates began to be used. This reduced the frequency dependence of the line, and now microstrip lines are often the preferred medium for microwave integrated circuits.

In this chapter we will study the properties of several types of transmission lines and waveguides that are in common use. As we know from Chapter 2, a transmission line is characterized by a propagation constant, an attenuation constant, and a characteristic impedance. These quantities will be derived by field theory analysis for the various lines and waveguides treated here.

We begin with a discussion of the different types of wave propagation and modes that can exist on general transmission lines and waveguides. Transmission lines that consist of two or more conductors may support *transverse electromagnetic* (TEM) waves, characterized by the lack of longitudinal field components. Such lines have a uniquely defined voltage, current, and characteristic impedance. Waveguides, often consisting of a single conductor, support *transverse electric* (TE) and/or *transverse magnetic* (TM) waves, characterized by the presence of longitudinal magnetic or electric field components. As we will see in Chapter 4, a unique definition of characteristic impedance is not possible for such waves, although definitions can be chosen so that the characteristic impedance concept can be extended to waveguides with meaningful results.

3.1

GENERAL SOLUTIONS FOR TEM, TE, AND TM WAVES

In this section we will find general solutions to Maxwell's equations for the specific cases of TEM, TE, and TM wave propagation in cylindrical transmission lines or waveguides. The geometry of an arbitrary transmission line or waveguide is shown in Figure 3.1 and is characterized by conductor boundaries that are parallel to the z -axis. These structures are assumed to be uniform in shape and dimension in the z direction and infinitely long. The conductors will initially be assumed to be perfectly conducting, but attenuation can be found by the perturbation method discussed in Chapter 2.

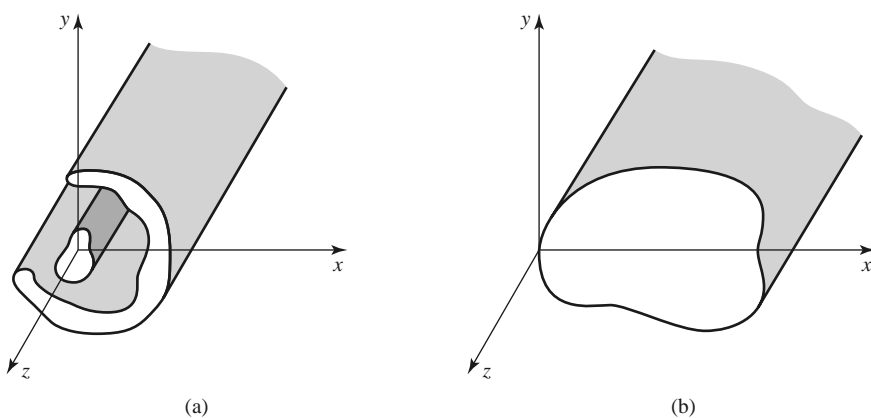


FIGURE 3.1 (a) General two-conductor transmission line and (b) closed waveguide.

We assume time-harmonic fields with an $e^{j\omega t}$ dependence and wave propagation along the z -axis. The electric and magnetic fields can then be written as

$$\bar{E}(x, y, z) = [\bar{e}(x, y) + \hat{z}e_z(x, y)]e^{-j\beta z}, \quad (3.1a)$$

$$\bar{H}(x, y, z) = [\bar{h}(x, y) + \hat{z}h_z(x, y)]e^{-j\beta z}, \quad (3.1b)$$

where $\bar{e}(x, y)$ and $\bar{h}(x, y)$ represent the transverse (\hat{x} , \hat{y}) electric and magnetic field components, and e_z and h_z are the longitudinal electric and magnetic field components. In (3.1) the wave is propagating in the $+z$ direction; $-z$ propagation can be obtained by replacing β with $-\beta$. In addition, if conductor or dielectric loss is present, the propagation constant will be complex; $j\beta$ should then be replaced with $\gamma = \alpha + j\beta$.

Assuming that the transmission line or waveguide region is source free, we can write Maxwell's equations as

$$\nabla \times \bar{E} = -j\omega\mu\bar{H}, \quad (3.2a)$$

$$\nabla \times \bar{H} = j\omega\epsilon\bar{E}. \quad (3.2b)$$

With an $e^{-j\beta z}$ z dependence, the three components of each of these vector equations can be reduced to the following:

$$\frac{\partial E_z}{\partial y} + j\beta E_y = -j\omega\mu H_x, \quad (3.3a)$$

$$-j\beta E_x - \frac{\partial E_z}{\partial x} = -j\omega\mu H_y, \quad (3.3b)$$

$$\frac{\partial E_y}{\partial x} - \frac{\partial E_x}{\partial y} = -j\omega\mu H_z, \quad (3.3c)$$

$$\frac{\partial H_z}{\partial y} + j\beta H_y = j\omega\epsilon E_x, \quad (3.4a)$$

$$-j\beta H_x - \frac{\partial H_z}{\partial x} = j\omega\epsilon E_y, \quad (3.4b)$$

$$\frac{\partial H_y}{\partial x} - \frac{\partial H_x}{\partial y} = j\omega\epsilon E_z. \quad (3.4c)$$

These six equations can be solved for the four transverse field components in terms of E_z and H_z [e.g., H_x can be derived by eliminating E_y from (3.3a) and (3.4b)] as follows:

$$H_x = \frac{j}{k_c^2} \left(\omega\epsilon \frac{\partial E_z}{\partial y} - \beta \frac{\partial H_z}{\partial x} \right), \quad (3.5a)$$

$$H_y = \frac{-j}{k_c^2} \left(\omega\epsilon \frac{\partial E_z}{\partial x} + \beta \frac{\partial H_z}{\partial y} \right), \quad (3.5b)$$

$$E_x = \frac{-j}{k_c^2} \left(\beta \frac{\partial E_z}{\partial x} + \omega\mu \frac{\partial H_z}{\partial y} \right), \quad (3.5c)$$

$$E_y = \frac{j}{k_c^2} \left(-\beta \frac{\partial E_z}{\partial y} + \omega\mu \frac{\partial H_z}{\partial x} \right), \quad (3.5d)$$

where

$$k_c^2 = k^2 - \beta^2 \quad (3.6)$$

is defined as the *cutoff wave number*; the reason for this terminology will become clear later. As in previous chapters,

$$k = \omega\sqrt{\mu\epsilon} = 2\pi/\lambda \quad (3.7)$$

is the wave number of the material filling the transmission line or waveguide region. If dielectric loss is present, ϵ can be made complex by using $\epsilon = \epsilon_0\epsilon_r(1 - j\tan\delta)$, where $\tan\delta$ is the loss tangent of the material.

Equations (3.5a)–(3.5d) are general results that can be applied to a variety of wave-guiding systems. We will now specialize these results to specific wave types.

TEM Waves

Transverse electromagnetic (TEM) waves are characterized by $E_z = H_z = 0$. Observe from (3.5) that if $E_z = H_z = 0$, then the transverse fields are also all zero, unless $k_c^2 = 0(k^2 = \beta^2)$, in which case we have an indeterminate result. However, we can return to (3.3)–(3.4) and apply the condition that $E_z = H_z = 0$. Then from (3.3a) and (3.4b), we can eliminate H_x to obtain

$$\beta^2 E_y = \omega^2 \mu\epsilon E_y,$$

or

$$\beta = \omega\sqrt{\mu\epsilon} = k, \quad (3.8)$$

as noted earlier. [This result can also be obtained from (3.3b) and (3.4a).] The cutoff wave number, $k_c = \sqrt{k^2 - \beta^2}$, is thus zero for TEM waves.

The Helmholtz wave equation for E_x is, from (1.42),

$$\left(\frac{\partial^2}{\partial x^2} + \frac{\partial^2}{\partial y^2} + \frac{\partial^2}{\partial z^2} + k^2 \right) E_x = 0, \quad (3.9)$$

but for $e^{-j\beta z}$ dependence, $(\partial^2/\partial z^2)E_x = -\beta^2 E_x = -k^2 E_x$, so (3.9) reduces to

$$\left(\frac{\partial^2}{\partial x^2} + \frac{\partial^2}{\partial y^2} \right) E_x = 0. \quad (3.10)$$

A similar result also applies to E_y , so using the form of \bar{E} assumed in (3.1a), we can write

$$\nabla_t^2 \bar{e}(x, y) = 0, \quad (3.11)$$

where $\nabla_t^2 = \partial^2/\partial x^2 + \partial^2/\partial y^2$ is the Laplacian operator in the two transverse dimensions.

The result of (3.11) shows that the transverse electric fields, $\bar{e}(x, y)$, of a TEM wave satisfy Laplace's equation. It is easy to show in the same way that the transverse magnetic fields also satisfy Laplace's equation:

$$\nabla_t^2 \bar{h}(x, y) = 0. \quad (3.12)$$

The transverse fields of a TEM wave are thus the same as the static fields that can exist between the conductors. In the electrostatic case, we know that the electric field can be expressed as the gradient of a scalar potential, $\Phi(x, y)$:

$$\bar{e}(x, y) = -\nabla_t \Phi(x, y), \quad (3.13)$$

where $\nabla_t = \hat{x}(\partial/\partial x) + \hat{y}(\partial/\partial y)$ is the transverse gradient operator in two dimensions. For the relation in (3.13) to be valid, the curl of \bar{e} must vanish, and this is indeed the case here since

$$\nabla_t \times \bar{e} = -j\omega\mu h_z \hat{z} = 0.$$

Using the fact that $\nabla \cdot \bar{D} = \epsilon \nabla_t \cdot \bar{e} = 0$ with (3.13) shows that $\Phi(x, y)$ also satisfies Laplace's equation,

$$\nabla_t^2 \Phi(x, y) = 0, \quad (3.14)$$

as expected from electrostatics. The voltage between two conductors can be found as

$$V_{12} = \Phi_1 - \Phi_2 = \int_1^2 \bar{E} \cdot d\bar{\ell}, \quad (3.15)$$

where Φ_1 and Φ_2 represent the potential at conductors 1 and 2, respectively. The current flow on a given conductor can be found from Ampere's law as

$$I = \oint_C \bar{H} \cdot d\bar{\ell}, \quad (3.16)$$

where C is the cross-sectional contour of the conductor.

TEM waves can exist when two or more conductors are present. Plane waves are also examples of TEM waves since there are no field components in the direction of propagation; in this case the transmission line conductors may be considered to be two infinitely large plates separated to infinity. The above results show that a closed conductor (such as a rectangular waveguide) cannot support TEM waves since the corresponding static potential in such a region would be zero (or possibly a constant), leading to $\bar{e} = 0$.

The wave impedance of a TEM mode can be found as the ratio of the transverse electric and magnetic fields:

$$Z_{\text{TEM}} = \frac{E_x}{H_y} = \frac{\omega\mu}{\beta} = \sqrt{\frac{\mu}{\epsilon}} = \eta, \quad (3.17a)$$

where (3.4a) was used. The other pair of transverse field components, from (3.3a), gives

$$Z_{\text{TEM}} = \frac{-E_y}{H_x} = \sqrt{\frac{\mu}{\epsilon}} = \eta. \quad (3.17b)$$

Combining the results of (3.17a) and (3.17b) gives a general expression for the transverse fields as

$$\bar{h}(x, y) = \frac{1}{Z_{\text{TEM}}} \hat{z} \times \bar{e}(x, y). \quad (3.18)$$

Note that the wave impedance is the same as that for a plane wave in a lossless medium, as derived in Chapter 1; the reader should not confuse this impedance with the characteristic impedance, Z_0 , of a transmission line. The latter relates traveling voltage and current and is a function of the line geometry as well as the material filling the line, while the wave impedance relates transverse field components and is dependent only on the material constants. From (2.32), the characteristic impedance of the TEM line is $Z_0 = V/I$, where V and I are the amplitudes of the incident voltage and current waves.

The procedure for analyzing a TEM line can be summarized as follows:

1. Solve Laplace's equation, (3.14), for $\Phi(x, y)$. The solution will contain several unknown constants.

2. Find these constants by applying the boundary conditions for the known voltages on the conductors.
3. Compute \bar{e} and \bar{E} from (3.13) and (3.1a). Compute \bar{h} and \bar{H} from (3.18) and (3.1b).
4. Compute V from (3.15) and I from (3.16).
5. The propagation constant is given by (3.8), and the characteristic impedance is given by $Z_0 = V/I$.

TE Waves

Transverse electric (TE) waves, (also referred to as H -waves) are characterized by $E_z = 0$ and $H_z \neq 0$. Equations (3.5) then reduce to

$$H_x = \frac{-j\beta}{k_c^2} \frac{\partial H_z}{\partial x}, \quad (3.19a)$$

$$H_y = \frac{-j\beta}{k_c^2} \frac{\partial H_z}{\partial y}, \quad (3.19b)$$

$$E_x = \frac{-j\omega\mu}{k_c^2} \frac{\partial H_z}{\partial y}, \quad (3.19c)$$

$$E_y = \frac{j\omega\mu}{k_c^2} \frac{\partial H_z}{\partial x}. \quad (3.19d)$$

In this case $k_c \neq 0$, and the propagation constant $\beta = \sqrt{k^2 - k_c^2}$ is generally a function of frequency and the geometry of the line or guide. To apply (3.19), one must first find H_z from the Helmholtz wave equation,

$$\left(\frac{\partial^2}{\partial x^2} + \frac{\partial^2}{\partial y^2} + \frac{\partial^2}{\partial z^2} + k^2 \right) H_z = 0, \quad (3.20)$$

which, since $H_z(x, y, z) = h_z(x, y)e^{-j\beta z}$, can be reduced to a two-dimensional wave equation for h_z :

$$\left(\frac{\partial^2}{\partial x^2} + \frac{\partial^2}{\partial y^2} + k_c^2 \right) h_z = 0, \quad (3.21)$$

since $k_c^2 = k^2 - \beta^2$. This equation must be solved subject to the boundary conditions of the specific guide geometry.

The TE wave impedance can be found as

$$Z_{TE} = \frac{E_x}{H_y} = \frac{-E_y}{H_x} = \frac{\omega\mu}{\beta} = \frac{k\eta}{\beta}, \quad (3.22)$$

which is seen to be frequency dependent. TE waves can be supported inside closed conductors, as well as between two or more conductors.

TM Waves

Transverse magnetic (TM) waves (also referred to as E -waves) are characterized by $E_z \neq 0$ and $H_z = 0$. Equations (3.5) then reduce to

$$H_x = \frac{j\omega\epsilon}{k_c^2} \frac{\partial E_z}{\partial y}, \quad (3.23a)$$

$$H_y = \frac{-j\omega\epsilon}{k_c^2} \frac{\partial E_z}{\partial x}, \quad (3.23b)$$

$$E_x = \frac{-j\beta}{k_c^2} \frac{\partial E_z}{\partial x}, \quad (3.23c)$$

$$E_y = \frac{-j\beta}{k_c^2} \frac{\partial E_z}{\partial y}. \quad (3.23d)$$

As in the TE case, $k_c \neq 0$, and the propagation constant $\beta = \sqrt{k^2 - k_c^2}$ is a function of frequency and the geometry of the line or guide. E_z is found from the Helmholtz wave equation,

$$\left(\frac{\partial^2}{\partial x^2} + \frac{\partial^2}{\partial y^2} + \frac{\partial^2}{\partial z^2} + k^2 \right) E_z = 0, \quad (3.24)$$

which, since $E_z(x, y, z) = e_z(x, y)e^{-j\beta z}$, can be reduced to a two-dimensional wave equation for e_z :

$$\left(\frac{\partial^2}{\partial x^2} + \frac{\partial^2}{\partial y^2} + k_c^2 \right) e_z = 0, \quad (3.25)$$

since $k_c^2 = k^2 - \beta^2$. This equation must be solved subject to the boundary conditions of the specific guide geometry.

The TM wave impedance can be found as

$$Z_{\text{TM}} = \frac{E_x}{H_y} = \frac{-E_y}{H_x} = \frac{\beta}{\omega\epsilon} = \frac{\beta\eta}{k}, \quad (3.26)$$

which is frequency dependent. As for TE waves, TM waves can be supported inside closed conductors, as well as between two or more conductors.

The procedure for analyzing TE and TM waveguides can be summarized as follows:

1. Solve the reduced Helmholtz equation, (3.21) or (3.25), for h_z or e_z . The solution will contain several unknown constants and the unknown cutoff wave number, k_c .
2. Use (3.19) or (3.23) to find the transverse fields from h_z or e_z .
3. Apply the boundary conditions to the appropriate field components to find the unknown constants and k_c .
4. The propagation constant is given by (3.6) and the wave impedance by (3.22) or (3.26).

Attenuation Due to Dielectric Loss

Attenuation in a transmission line or waveguide can be caused by either dielectric loss or conductor loss. If α_d is the attenuation constant due to dielectric loss and α_c is the attenuation constant due to conductor loss, then the total attenuation constant is $\alpha = \alpha_d + \alpha_c$.

Attenuation caused by conductor loss can be calculated using the perturbation method of Section 2.7; this loss depends on the field distribution in the guide and so must be evaluated separately for each type of transmission line or waveguide. However, if the line or guide is completely filled with a homogeneous dielectric, the attenuation due to a lossy dielectric material can be calculated from the propagation constant, and this result will apply to any guide or line with a homogeneous dielectric filling.

Thus, use of the complex permittivity allows the complex propagation constant to be written as

$$\begin{aligned} \gamma &= \alpha_d + j\beta = \sqrt{k_c^2 - k^2} \\ &= \sqrt{k_c^2 - \omega^2\mu_0\epsilon_0\epsilon_r(1 - j\tan\delta)}. \end{aligned} \quad (3.27)$$

In practice, most dielectric materials have small losses ($\tan \delta \ll 1$), and so this expression can be simplified by using the first two terms of the Taylor expansion,

$$\sqrt{a^2 + x^2} \simeq a + \frac{1}{2} \left(\frac{x^2}{a} \right), \quad \text{for } x \ll a.$$

Then (3.27) reduces to

$$\begin{aligned} \gamma &= \sqrt{k_c^2 - k^2 + jk^2 \tan \delta} \\ &\simeq \sqrt{k_c^2 - k^2} + \frac{jk^2 \tan \delta}{2\sqrt{k_c^2 - k^2}} \\ &= \frac{k^2 \tan \delta}{2\beta} + j\beta, \end{aligned} \quad (3.28)$$

since $\sqrt{k_c^2 - k^2} = j\beta$. In these results, $k = \omega\sqrt{\mu_0\epsilon_0\epsilon_r}$ is the (real) wave number in the absence of loss. Equation (3.28) shows that when the loss is small the phase constant β is unchanged, while the attenuation constant due to dielectric loss is given by

$$\alpha_d = \frac{k^2 \tan \delta}{2\beta} \text{ Np/m (TE or TM waves).} \quad (3.29)$$

This result applies to any TE or TM wave, as long as the guide is completely filled with the dielectric material. It can also be used for TEM lines, where $k_c = 0$, by letting $\beta = k$:

$$\alpha_d = \frac{k \tan \delta}{2} \text{ Np/m (TEM waves).} \quad (3.30)$$

3.2

PARALLEL PLATE WAVEGUIDE

The parallel plate waveguide is the simplest type of guide that can support TM and TE modes; it can also support a TEM mode since it is formed from two flat conducting plates, or strips, as shown in Figure 3.2. Although it is an idealization, understanding the parallel plate guide can be useful because its operation is similar to that of many other waveguides. The parallel plate guide can also be useful for modeling the propagation of higher order modes in stripline.

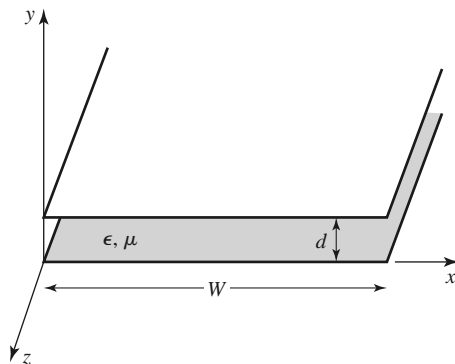


FIGURE 3.2 Geometry of a parallel plate waveguide.

In the geometry of the parallel plate waveguide of Figure 3.2, the strip width, W , is assumed to be much greater than the separation, d , so that fringing fields and any x variation can be ignored. A material with permittivity ϵ and permeability μ is assumed to fill the region between the two plates. We will derive solutions for TEM, TM, and TE waves.

TEM Modes

As discussed in Section 3.1, the TEM mode solution can be obtained by solving Laplace's equation, (3.14), for the electrostatic potential $\Phi(x, y)$ between the two plates. Thus,

$$\nabla_t^2 \Phi(x, y) = 0, \quad \text{for } 0 \leq x \leq W, \quad 0 \leq y \leq d. \quad (3.31)$$

If we assume that the bottom plate is at ground (zero) potential and the top plate at a potential of V_o , then the boundary conditions for $\Phi(x, y)$ are

$$\Phi(x, 0) = 0, \quad (3.32a)$$

$$\Phi(x, d) = V_o. \quad (3.32b)$$

Because there is no variation in x , the general solution to (3.31) for $\Phi(x, y)$ is

$$\Phi(x, y) = A + By,$$

and the constants A, B can be evaluated from the boundary conditions of (3.32) to give the final solution as

$$\Phi(x, y) = V_o y/d. \quad (3.33)$$

The transverse electric field is, from (3.13),

$$\bar{e}(x, y) = -\nabla_t \Phi(x, y) = -\hat{y} \frac{V_o}{d}, \quad (3.34)$$

so that the total electric field is

$$\bar{E}(x, y, z) = \bar{e}(x, y) e^{-j k z} = -\hat{y} \frac{V_o}{d} e^{-j k z}, \quad (3.35)$$

where $k = \omega \sqrt{\mu \epsilon}$ is the propagation constant of the TEM wave, as in (3.8). The magnetic field, from (3.18), is

$$\bar{H}(x, y, z) = \bar{h}(x, y) e^{-j k z} = \frac{1}{\eta} \hat{z} \times \bar{E}(x, y, z) = \hat{x} \frac{V_o}{\eta d} e^{-j k z}, \quad (3.36)$$

where $\eta = \sqrt{\mu/\epsilon}$ is the intrinsic impedance of the medium between the parallel plates. Note that $E_z = H_z = 0$ and that the fields are similar in form to a plane wave in a homogeneous region.

The voltage of the top plate with respect to the bottom plate can be calculated from (3.15) and (3.35) as

$$V = - \int_{y=0}^d E_y dy = V_o e^{-j k z}, \quad (3.37)$$

as expected. The total current on the top plate can be found from Ampere's law or the surface current density:

$$I = \int_{x=0}^W \bar{J}_s \cdot \hat{z} dx = \int_{x=0}^W (-\hat{y} \times \bar{H}) \cdot \hat{z} dx = \int_{x=0}^W H_x dx = \frac{W V_o}{\eta d} e^{-jkz}. \quad (3.38)$$

Then the characteristic impedance is

$$Z_0 = \frac{V}{I} = \frac{\eta d}{W}, \quad (3.39)$$

which is seen to be a constant dependent only on the geometry and material parameters of the guide. The phase velocity is also a constant:

$$v_p = \frac{\omega}{\beta} = \frac{1}{\sqrt{\mu\epsilon}}, \quad (3.40)$$

which is the speed of light in the material medium.

Attenuation due to dielectric loss is given by (3.30). The formula for conductor attenuation will be derived in the next subsection as a special case of TM mode attenuation.

TM Modes

As discussed in Section 3.1, TM waves are characterized by $H_z = 0$ and a nonzero E_z field that satisfies the reduced wave equation of (3.25), with $\partial/\partial x = 0$:

$$\left(\frac{\partial^2}{\partial y^2} + k_c^2 \right) e_z(x, y) = 0, \quad (3.41)$$

where $k_c = \sqrt{k^2 - \beta^2}$ is the cutoff wave number, and $E_z(x, y, z) = e_z(x, y) e^{-j\beta z}$. The general solution to (3.41) is of the form

$$e_z(x, y) = A \sin k_c y + B \cos k_c y, \quad (3.42)$$

subject to the boundary conditions that

$$e_z(x, y) = 0, \quad \text{at } y = 0, d. \quad (3.43)$$

This implies that $B = 0$ and $k_c d = n\pi$ for $n = 0, 1, 2, 3, \dots$, or

$$k_c = \frac{n\pi}{d}, \quad n = 0, 1, 2, 3, \dots \quad (3.44)$$

Thus the cutoff wave number, k_c , is constrained to discrete values as given by (3.44); this implies that the propagation constant, β , is given by

$$\beta = \sqrt{k^2 - k_c^2} = \sqrt{k^2 - (n\pi/d)^2}. \quad (3.45)$$

The solution for $e_z(x, y)$ is then

$$e_z(x, y) = A_n \sin \frac{n\pi y}{d}, \quad (3.46)$$

and thus,

$$E_z(x, y, z) = A_n \sin \frac{n\pi y}{d} e^{-j\beta z}. \quad (3.47)$$

The transverse field components can be found, using (3.23), to be

$$H_x = \frac{j\omega\epsilon}{k_c} A_n \cos \frac{n\pi y}{d} e^{-j\beta z}, \quad (3.48a)$$

$$E_y = \frac{-j\beta}{k_c} A_n \cos \frac{n\pi y}{d} e^{-j\beta z}, \quad (3.48b)$$

$$E_x = H_y = 0. \quad (3.48c)$$

Observe that for $n = 0$, $\beta = k = \omega\sqrt{\mu\epsilon}$, and that $E_z = 0$. The E_y and H_x fields are then constant in y , so that the TM_0 mode is actually identical to the TEM mode. For $n > 0$, however, the situation is different. Each value of n corresponds to a different TM mode, denoted as the TM_n mode, and each mode has its own propagation constant given by (3.45) and field expressions given by (3.48).

From (3.45) it can be seen that β is real only when $k > k_c$. Because $k = \omega\sqrt{\mu\epsilon}$ is proportional to frequency, the TM_n modes (for $n > 0$) exhibit a cutoff phenomenon, whereby no propagation will occur until the frequency is such that $k > k_c$. The *cutoff frequency* of the TM_n mode can be found as

$$f_c = \frac{k_c}{2\pi\sqrt{\mu\epsilon}} = \frac{n}{2d\sqrt{\mu\epsilon}}. \quad (3.49)$$

Thus, the TM mode (for $n > 0$) that propagates at the lowest frequency is the TM_1 mode, with a cutoff frequency of $f_c = 1/2d\sqrt{\mu\epsilon}$; the TM_2 mode has a cutoff frequency equal to twice this value, and so on. At frequencies below the cutoff frequency of a given mode, the propagation constant is purely imaginary, corresponding to a rapid exponential decay of the fields. Such modes are referred to as *cutoff modes*, or *evanescent modes*. Because of the cutoff frequency, below which propagation cannot occur, waveguide mode propagation is analogous to a high-pass filter response.

The wave impedance of a TM mode, from (3.26), is a function of frequency:

$$Z_{\text{TM}} = \frac{-E_y}{H_x} = \frac{\beta}{\omega\epsilon} = \frac{\beta\eta}{k}, \quad (3.50)$$

which we see is pure real when $f > f_c$ but pure imaginary when $f < f_c$. The phase velocity is also a function of frequency:

$$v_p = \frac{\omega}{\beta}, \quad (3.51)$$

and is seen to be greater than $1/\sqrt{\mu\epsilon} = \omega/k$, the speed of light in the medium, since $\beta < k$. The guide wavelength is defined as

$$\lambda_g = \frac{2\pi}{\beta}, \quad (3.52)$$

and is the distance between equiphase planes along the z -axis. Note that $\lambda_g > \lambda = 2\pi/k$, the wavelength of a plane wave in the material. The phase velocity and guide wavelength are defined only for a propagating mode, for which β is real. One may also define a *cutoff wavelength* for the TM_n mode as

$$\lambda_c = \frac{2d}{n}. \quad (3.53)$$

It is instructive to compute the Poynting vector to see how power propagates in the TM_n mode. From (1.91), the time-average power passing a transverse cross section of the parallel plate guide is

$$P_o = \frac{1}{2} \text{Re} \int_{x=0}^W \int_{y=0}^d \bar{E} \times \bar{H}^* \cdot \hat{z} dy dx = -\frac{1}{2} \text{Re} \int_{x=0}^W \int_{y=0}^d E_y H_x^* dy dx$$

$$= \frac{W \text{Re}(\beta) \omega \epsilon}{2k_c^2} |A_n|^2 \int_{y=0}^d \cos^2 \frac{n\pi y}{d} dy = \begin{cases} \frac{W \text{Re}(\beta) \omega \epsilon d}{4k_c^2} |A_n|^2 & \text{for } n > 0 \\ \frac{W \text{Re}(\beta) \omega \epsilon d}{2k_c^2} |A_n|^2 & \text{for } n = 0 \end{cases} \quad (3.54)$$

where (3.48a, b) were used for E_y, H_x . Thus, P_o is positive and nonzero when β is real, which occurs when $f > f_c$. When the mode is below cutoff, β is imaginary, and then $P_o = 0$.

TM (or TE) waveguide mode propagation has an interesting interpretation when viewed as a pair of bouncing plane waves. For example, consider the dominant TM_1 mode, which has propagation constant

$$\beta_1 = \sqrt{k^2 - (\pi/d)^2}, \quad (3.55)$$

and E_z field

$$E_z = A_1 \sin \frac{\pi y}{d} e^{-j\beta_1 z},$$

which can be rewritten as

$$E_z = \frac{A_1}{2j} \left[e^{j(\pi y/d - \beta_1 z)} - e^{-j(\pi y/d + \beta_1 z)} \right]. \quad (3.56)$$

This result is in the form of two plane waves traveling obliquely in the $-y, +z$ and $+y, +z$ directions, respectively, as shown in Figure 3.3. By comparison with the phase factor of (1.132), the angle θ that each plane wave makes with the z -axis satisfies the relations

$$k \sin \theta = \frac{\pi}{d}, \quad (3.57a)$$

$$k \cos \theta = \beta_1, \quad (3.57b)$$

so that $(\pi/d)^2 + \beta_1^2 = k^2$, as in (3.55). For $f > f_c$, β is real and less than k_1 , so θ is some angle between 0° and 90° , and the mode can be thought of as two plane waves alternately bouncing off of the top and bottom plates.

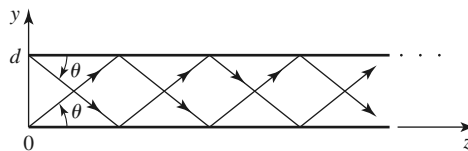


FIGURE 3.3 Bouncing plane wave interpretation of the TM_1 parallel plate waveguide mode.

The phase velocity of each plane wave along its direction of propagation (θ direction) is $\omega/k = 1/\sqrt{\mu\epsilon}$, which is the speed of light in the material filling the guide. However, the phase velocity of the plane waves in the z direction is $\omega/\beta_1 = 1/\sqrt{\mu\epsilon} \cos \theta$, which is greater than the speed of light in the material. (This situation is analogous to ocean waves hitting a shoreline: the intersection point of the shore and an obliquely incident wave crest moves faster than the wave crest itself.) The superposition of the two plane wave fields is such that complete cancellation occurs at $y = 0$ and $y = d$, to satisfy the boundary condition that $E_z = 0$ at these planes. As f decreases to f_c , β_1 approaches zero, so that, by (3.57b), θ approaches 90° . The two plane waves are then bouncing up and down, with no motion in the $+z$ direction, and no real power flow occurs in the z direction.

Attenuation due to dielectric loss can be found from (3.29). Conductor loss can be treated using the perturbation method. Thus,

$$\alpha_c = \frac{P_\ell}{2P_o}, \quad (3.58)$$

where P_o is the power flow down the guide in the absence of conductor loss, as given by (3.54). P_ℓ is the power dissipated per unit length in the two lossy conductors and can be found from (2.97) as

$$P_\ell = 2 \left(\frac{R_s}{2} \right) \int_{x=0}^W |\bar{J}_s|^2 dx = \frac{\omega^2 \epsilon^2 R_s W}{k_c^2} |A_n|^2, \quad (3.59)$$

where R_s is the surface resistivity of the conductors. Using (3.54) and (3.59) in (3.58) gives the attenuation due to conductor loss as

$$\alpha_c = \frac{2\omega\epsilon R_s}{\beta d} = \frac{2k R_s}{\beta \eta d} \text{ Np/m}, \quad \text{for } n > 0. \quad (3.60)$$

As discussed previously, the TEM mode is identical to the TM_0 mode for the parallel plate waveguide, so the above attenuation results for the TM_n mode can be used to obtain the TEM mode attenuation by letting $n = 0$. For this case, the $n = 0$ result of (3.54) must be used in (3.58), to obtain

$$\alpha_c = \frac{R_s}{\eta d} \text{ Np/m}. \quad (3.61)$$

TE Modes

TE modes, characterized by $E_z = 0$, can also propagate in a parallel plate waveguide. From (3.21), with $\partial/\partial x = 0$, H_z must satisfy the reduced wave equation,

$$\left(\frac{\partial^2}{\partial y^2} + k_c^2 \right) h_z(x, y) = 0, \quad (3.62)$$

where $k_c = \sqrt{k^2 - \beta^2}$ is the cutoff wave number and $H_z(x, y, z) = h_z(x, y) e^{-j\beta z}$. The general solution to (3.62) is

$$h_z(x, y) = A \sin k_c y + B \cos k_c y. \quad (3.63)$$

The boundary conditions are that $E_x = 0$ at $y = 0, d$; E_z is identically zero for TE modes. From (3.19c) we have

$$E_x = \frac{-j\omega\mu}{k_c} (A \cos k_c y - B \sin k_c y) e^{-j\beta z}, \quad (3.64)$$

and applying the boundary conditions shows that $A = 0$ and

$$k_c = \frac{n\pi}{d}, \quad n = 1, 2, 3 \dots, \quad (3.65)$$

as for the TM case. The final solution for H_z is then

$$H_z(x, y) = B_n \cos \frac{n\pi y}{d} e^{-j\beta z}. \quad (3.66)$$

The transverse fields can be computed from (3.19) as

$$E_x = \frac{j\omega\mu}{k_c} B_n \sin \frac{n\pi y}{d} e^{-j\beta z}, \quad (3.67a)$$

$$H_y = \frac{j\beta}{k_c} B_n \sin \frac{n\pi y}{d} e^{-j\beta z}, \quad (3.67b)$$

$$E_y = H_x = 0. \quad (3.67c)$$

The propagation constant of the TE_n mode is given as

$$\beta = \sqrt{k^2 - \left(\frac{n\pi}{d}\right)^2}, \quad (3.68)$$

which is the same as the propagation constant of the TM_n mode. The cutoff frequency of the TE_n mode is

$$f_c = \frac{n}{2d\sqrt{\mu\epsilon}}, \quad (3.69)$$

which is also identical to that of the TM_n mode. The wave impedance of the TE_n mode is, from (3.22),

$$Z_{\text{TE}} = \frac{E_x}{H_y} = \frac{\omega\mu}{\beta} = \frac{k\eta}{\beta}, \quad (3.70)$$

which is seen to be real for propagating modes and imaginary for nonpropagating, or cutoff, modes. The phase velocity, guide wavelength, and cutoff wavelength are similar to the results obtained for the TM modes.

The power flow down the guide for a TE_n mode can be calculated as

$$\begin{aligned} P_o &= \frac{1}{2} \text{Re} \int_{x=0}^W \int_{y=0}^d \bar{E} \times \bar{H}^* \cdot \hat{z} dy dx = \frac{1}{2} \text{Re} \int_{x=0}^W \int_{y=0}^d E_x H_y^* dy dx \\ &= \frac{\omega\mu d W}{4k_c^2} |B_n|^2 \text{Re}(\beta), \quad \text{for } n > 0, \end{aligned} \quad (3.71)$$

which is zero if the operating frequency is below the cutoff frequency (β imaginary).

Note that if $n = 0$, then $E_x = H_y = 0$ from (3.67), and thus $P_o = 0$, implying that there is no TE_0 mode.

Attenuation can be calculated in the same way as for the TM modes. The attenuation due to dielectric loss is given by (3.29). It is left as a problem to show that the attenuation due to conductor loss for TE modes is given by

$$\alpha_c = \frac{2k_c^2 R_s}{\omega\mu\beta d} = \frac{2k_c^2 R_s}{k\beta\eta d} \text{ Np/m.} \quad (3.72)$$

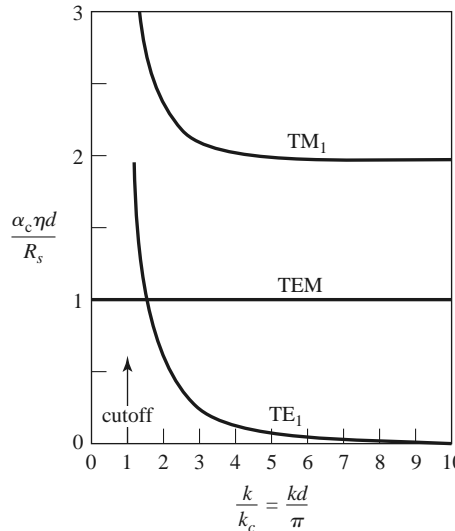


FIGURE 3.4 Attenuation due to conductor loss for the TEM, TM₁, and TE₁ modes of a parallel plate waveguide.

Figure 3.4 shows attenuation versus frequency due to conductor loss for the TEM, TM₁, and TE₁ modes. Observe that $\alpha_c \rightarrow \infty$ as cutoff is approached for the TM and TE modes.

Table 3.1 summarizes a number of useful results for parallel plate waveguide modes. Field lines for the TEM, TM₁, and TE₁ modes are shown in Figure 3.5.

TABLE 3.1 Summary of Results for Parallel Plate Waveguide

Quantity	TEM Mode	TM _n Mode	TE _n Mode
k	$\omega\sqrt{\mu\epsilon}$	$\omega\sqrt{\mu\epsilon}$	$\omega\sqrt{\mu\epsilon}$
k_c	0	$n\pi/d$	$n\pi/d$
β	$k = \omega\sqrt{\mu\epsilon}$	$\sqrt{k^2 - k_c^2}$	$\sqrt{k^2 - k_c^2}$
λ_c	∞	$2\pi/k_c = 2d/n$	$2\pi/k_c = 2d/n$
λ_g	$2\pi/k$	$2\pi/\beta$	$2\pi/\beta$
v_p	$\omega/k = 1/\sqrt{\mu\epsilon}$	ω/β	ω/β
α_d	$(k \tan \delta)/2$	$(k^2 \tan \delta)/2\beta$	$(k^2 \tan \delta)/2\beta$
α_c	$R_s/\eta d$	$2kR_s/\beta\eta d$	$2k_c^2 R_s/k\beta\eta d$
E_z	0	$A \sin(n\pi y/d) e^{-j\beta z}$	0
H_z	0	0	$B \cos(n\pi y/d) e^{-j\beta z}$
E_x	0	0	$(j\omega\mu/k_c)B \sin(n\pi y/d) e^{-j\beta z}$
E_y	$(-V_o/d)e^{-j\beta z}$	$(-j\beta/k_c)A \cos(n\pi y/d) e^{-j\beta z}$	0
H_x	$(V_o/\eta d)e^{-j\beta z}$	$(j\omega\epsilon/k_c)A \cos(n\pi y/d) e^{-j\beta z}$	0
H_y	0	0	$(j\beta/k_c)B_n \sin(n\pi y/d) e^{-j\beta z}$
Z	$Z_{\text{TEM}} = \eta d/W$	$Z_{\text{TM}} = \beta\eta/k$	$Z_{\text{TE}} = k\eta/\beta$

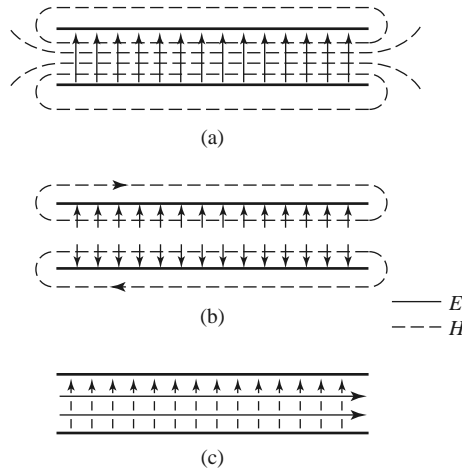


FIGURE 3.5 Field lines for the (a) TEM, (b) TM₁, and (c) TE₁ modes of a parallel plate waveguide. There is no variation across the width of the waveguide.

3.3 RECTANGULAR WAVEGUIDE

Rectangular waveguides were one of the earliest types of transmission lines used to transport microwave signals, and they are still used for many applications. A large variety of components such as couplers, detectors, isolators, attenuators, and slotted lines are commercially available for various standard waveguide bands from 1 to 220 GHz. Figure 3.6 shows some of the standard rectangular waveguide components that are available. Because of the trend toward miniaturization and integration, most modern microwave circuitry is fabricated using planar transmission lines such as microstrips and stripline rather than waveguides. There is, however, still a need for waveguides in many cases, including high-power systems, millimeter wave applications, satellite systems, and some precision test applications.

The hollow rectangular waveguide can propagate TM and TE modes but not TEM waves since only one conductor is present. We will see that the TM and TE modes of a rectangular waveguide have cutoff frequencies below which propagation is not possible, similar to the TM and TE modes of the parallel plate guide.

TE Modes

The geometry of a rectangular waveguide is shown in Figure 3.7, where it is assumed that the guide is filled with a material of permittivity ϵ and permeability μ . It is standard convention to have the longest side of the waveguide along the x -axis, so that $a > b$.

TE waveguide modes are characterized by fields with $E_z = 0$, while H_z must satisfy the reduced wave equation of (3.21):

$$\left(\frac{\partial^2}{\partial x^2} + \frac{\partial^2}{\partial y^2} + k_c^2 \right) h_z(x, y) = 0, \quad (3.73)$$

with $H_z(x, y, z) = h_z(x, y)e^{-j\beta z}$; here $k_c = \sqrt{k^2 - \beta^2}$ is the cutoff wave number. The partial differential equation (3.73) can be solved by the method of separation of variables by letting

$$h_z(x, y) = X(x)Y(y) \quad (3.74)$$

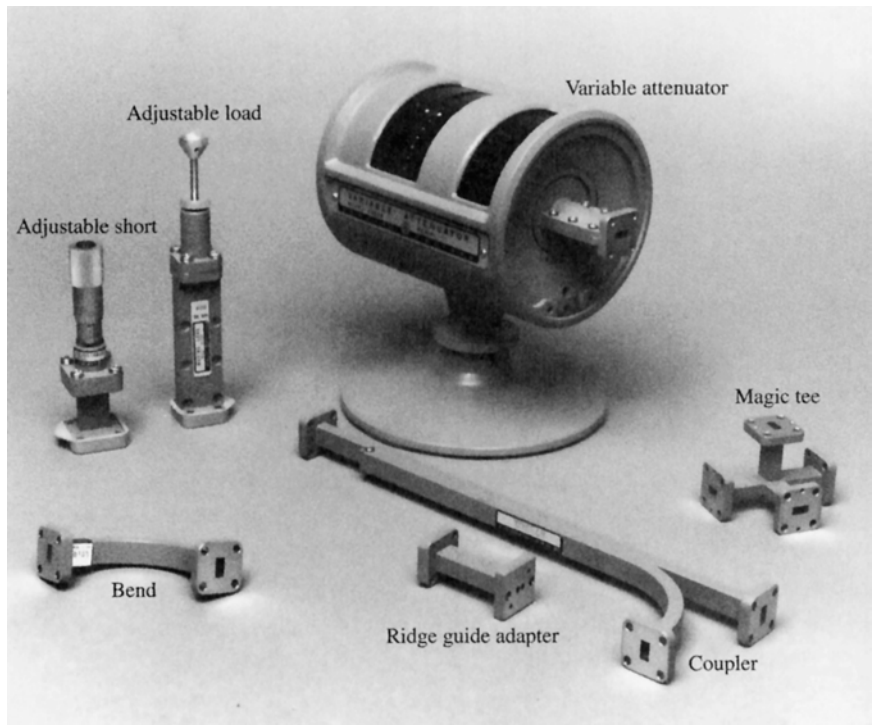


FIGURE 3.6 Photograph of Ka-band (WR-28) rectangular waveguide components. Clockwise from top: a variable attenuator, an E-H (magic) tee junction, a directional coupler, an adaptor to ridge waveguide, an E-plane swept bend, an adjustable short, and a sliding matched load.

and substituting into (3.73) to obtain

$$\frac{1}{X} \frac{d^2X}{dx^2} + \frac{1}{Y} \frac{d^2Y}{dy^2} + k_c^2 = 0. \quad (3.75)$$

Then, by the usual separation-of-variables argument (see Section 1.5), each of the terms in (3.75) must be equal to a constant, so we define separation constants k_x and k_y such that

$$\frac{d^2X}{dx^2} + k_x^2 X = 0, \quad (3.76a)$$

$$\frac{d^2Y}{dy^2} + k_y^2 Y = 0, \quad (3.76b)$$

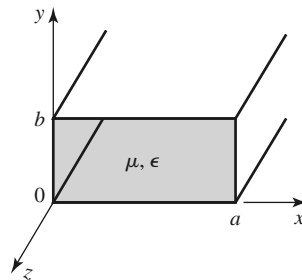


FIGURE 3.7 Geometry of a rectangular waveguide.

and

$$k_x^2 + k_y^2 = k_c^2. \quad (3.77)$$

The general solution for h_z can then be written as

$$h_z(x, y) = (A \cos k_x x + B \sin k_x x)(C \cos k_y y + D \sin k_y y). \quad (3.78)$$

To evaluate the constants in (3.78) we must apply the boundary conditions on the electric field components tangential to the waveguide walls. That is,

$$e_x(x, y) = 0, \quad \text{at } y = 0, b, \quad (3.79a)$$

$$e_y(x, y) = 0, \quad \text{at } x = 0, a. \quad (3.79b)$$

We therefore cannot use h_z of (3.78) directly but must first use (3.19c) and (3.19d) to find e_x and e_y from h_z :

$$e_x = \frac{-j\omega\mu}{k_c^2} k_y (A \cos k_x x + B \sin k_x x) (-C \sin k_y y + D \cos k_y y), \quad (3.80a)$$

$$e_y = \frac{j\omega\mu}{k_c^2} k_x (-A \sin k_x x + B \cos k_x x) (C \cos k_y y + D \sin k_y y). \quad (3.80b)$$

Then from (3.79a) and (3.80a) we see that $D = 0$, and $k_y = n\pi/b$ for $n = 0, 1, 2, \dots$. From (3.79b) and (3.80b) we have that $B = 0$ and $k_x = m\pi/a$ for $m = 0, 1, 2, \dots$. The final solution for H_z is then

$$H_z(x, y, z) = A_{mn} \cos \frac{m\pi x}{a} \cos \frac{n\pi y}{b} e^{-j\beta z}, \quad (3.81)$$

where A_{mn} is an arbitrary amplitude constant composed of the remaining constants A and C of (3.78).

The transverse field components of the TE_{mn} mode can be found using (3.19) and (3.81):

$$E_x = \frac{j\omega\mu n\pi}{k_c^2 b} A_{mn} \cos \frac{m\pi x}{a} \sin \frac{n\pi y}{b} e^{-j\beta z}, \quad (3.82a)$$

$$E_y = \frac{-j\omega\mu m\pi}{k_c^2 a} A_{mn} \sin \frac{m\pi x}{a} \cos \frac{n\pi y}{b} e^{-j\beta z}, \quad (3.82b)$$

$$H_x = \frac{j\beta m\pi}{k_c^2 a} A_{mn} \sin \frac{m\pi x}{a} \cos \frac{n\pi y}{b} e^{-j\beta z}, \quad (3.82c)$$

$$H_y = \frac{j\beta n\pi}{k_c^2 b} A_{mn} \cos \frac{m\pi x}{a} \sin \frac{n\pi y}{b} e^{-j\beta z}. \quad (3.82d)$$

The propagation constant is

$$\beta = \sqrt{k^2 - k_c^2} = \sqrt{k^2 - \left(\frac{m\pi}{a}\right)^2 - \left(\frac{n\pi}{b}\right)^2}, \quad (3.83)$$

which is seen to be real, corresponding to a propagating mode, when

$$k > k_c = \sqrt{\left(\frac{m\pi}{a}\right)^2 + \left(\frac{n\pi}{b}\right)^2}.$$

Each mode (each combination of m and n) has a cutoff frequency $f_{c_{mn}}$ given by

$$f_{c_{mn}} = \frac{k_c}{2\pi\sqrt{\mu\epsilon}} = \frac{1}{2\pi\sqrt{\mu\epsilon}} \sqrt{\left(\frac{m\pi}{a}\right)^2 + \left(\frac{n\pi}{b}\right)^2}. \quad (3.84)$$

The mode with the lowest cutoff frequency is called the dominant mode; because we have assumed $a > b$, the lowest cutoff frequency occurs for the TE_{10} ($m = 1, n = 0$) mode:

$$f_{c_{10}} = \frac{1}{2a\sqrt{\mu\epsilon}}. \quad (3.85)$$

Thus the TE_{10} mode is the dominant TE mode and, as we will see, the overall dominant mode of the rectangular waveguide. Observe that the field expressions for \bar{E} and \bar{H} in (3.82) are all zero if both $m = n = 0$; there is no TE_{00} mode.

At a given operating frequency f only those modes having $f > f_c$ will propagate; modes with $f < f_c$ will lead to an imaginary β (or real α), meaning that all field components will decay exponentially away from the source of excitation. Such modes are referred to as *cutoff modes*, or *evanescent modes*. If more than one mode is propagating, the waveguide is said to be *overmoded*.

From (3.22) the wave impedance that relates the transverse electric and magnetic fields is

$$Z_{\text{TE}} = \frac{E_x}{H_y} = \frac{-E_y}{H_x} = \frac{k\eta}{\beta}, \quad (3.86)$$

where $\eta = \sqrt{\mu/\epsilon}$ is the intrinsic impedance of the material filling the waveguide. Note that Z_{TE} is real when β is real (a propagating mode) but is imaginary when β is imaginary (a cutoff mode).

The guide wavelength is defined as the distance between two equal-phase planes along the waveguide and is equal to

$$\lambda_g = \frac{2\pi}{\beta} > \frac{2\pi}{k} = \lambda, \quad (3.87)$$

which is thus greater than λ , the wavelength of a plane wave in the medium filling the guide. The phase velocity is

$$v_p = \frac{\omega}{\beta} > \frac{\omega}{k} = 1/\sqrt{\mu\epsilon}, \quad (3.88)$$

which is greater than $1/\sqrt{\mu\epsilon}$, the speed of light (plane wave) in the medium.

In the vast majority of waveguide applications the operating frequency and guide dimensions are chosen so that only the dominant TE_{10} mode will propagate. Because of the practical importance of the TE_{10} mode, we will list the field components and derive the attenuation due to conductor loss for this case.

Specializing (3.81) and (3.82) to the $m = 1, n = 0$ case gives the following results for the TE_{10} mode fields:

$$H_z = A_{10} \cos \frac{\pi x}{a} e^{-j\beta z}, \quad (3.89a)$$

$$E_y = \frac{-j\omega\mu a}{\pi} A_{10} \sin \frac{\pi x}{a} e^{-j\beta z}, \quad (3.89b)$$

$$H_x = \frac{j\beta a}{\pi} A_{10} \sin \frac{\pi x}{a} e^{-j\beta z}, \quad (3.89c)$$

$$E_x = E_z = H_y = 0. \quad (3.89d)$$

The cutoff wave number and propagation constant for the TE₁₀ mode are, respectively,

$$k_c = \pi/a, \quad (3.90)$$

$$\beta = \sqrt{k^2 - (\pi/a)^2}. \quad (3.91)$$

The power flow down the guide for the TE₁₀ mode can be calculated as

$$\begin{aligned} P_{10} &= \frac{1}{2} \operatorname{Re} \int_{x=0}^a \int_{y=0}^b \bar{E} \times \bar{H}^* \cdot \hat{z} dy dx \\ &= \frac{1}{2} \operatorname{Re} \int_{x=0}^a \int_{y=0}^b E_y H_x^* dy dx \\ &= \frac{\omega \mu a^2}{2\pi^2} \operatorname{Re}(\beta) |A_{10}|^2 \int_{x=0}^a \int_{y=0}^b \sin^2 \frac{\pi x}{a} dy dx \\ &= \frac{\omega \mu a^3 |A_{10}|^2 b}{4\pi^2} \operatorname{Re}(\beta). \end{aligned} \quad (3.92)$$

Note that this result gives nonzero real power only when β is real, corresponding to a propagating mode.

Attenuation in a rectangular waveguide may occur due to dielectric loss or conductor loss. Dielectric loss can be treated by making ϵ complex and using the general result given in (3.29). Conductor loss is best treated using the perturbation method. The power lost per unit length due to finite wall conductivity is, from (1.131),

$$P_\ell = \frac{R_s}{2} \int_C |\bar{J}_s|^2 d\ell, \quad (3.93)$$

where R_s is the wall surface resistance, and the integration contour C encloses the inside perimeter of the guide walls. There are surface currents on all four walls, but from symmetry the currents on the top and bottom walls are identical, as are the currents on the left and right side walls. So we can compute the power lost in the walls at $x = 0$ and $y = 0$ and double their sum to obtain the total power loss. The surface current on the $x = 0$ (left) wall is

$$\bar{J}_s = \hat{n} \times \bar{H}|_{x=0} = \hat{x} \times \hat{z} H_z|_{x=0} = -\hat{y} H_z|_{x=0} = -\hat{y} A_{10} e^{-j\beta z}, \quad (3.94a)$$

and the surface current on the $y = 0$ (bottom) wall is

$$\begin{aligned} \bar{J}_s &= \hat{n} \times \bar{H}|_{y=0} = \hat{y} \times (\hat{x} H_x|_{y=0} + \hat{z} H_z|_{y=0}) \\ &= -\hat{z} \frac{j\beta a}{\pi} A_{10} \sin \frac{\pi x}{a} e^{-j\beta z} + \hat{x} A_{10} \cos \frac{\pi x}{a} e^{-j\beta z}. \end{aligned} \quad (3.94b)$$

Substituting (3.94) into (3.93) gives

$$\begin{aligned} P_\ell &= R_s \int_{y=0}^b |J_{sy}|^2 dy + R_s \int_{x=0}^a \left[|J_{sx}|^2 + |J_{sz}|^2 \right] dx \\ &= R_s |A_{10}|^2 \left(b + \frac{a}{2} + \frac{\beta^2 a^3}{2\pi^2} \right). \end{aligned} \quad (3.95)$$

The attenuation due to conductor loss for the TE₁₀ mode is then

$$\begin{aligned}\alpha_c &= \frac{P_\ell}{2P_{10}} = \frac{2\pi^2 R_s (b + a/2 + \beta^2 a^3 / 2\pi^2)}{\omega \mu a^3 b \beta} \\ &= \frac{R_s}{a^3 b \beta k \eta} (2b\pi^2 + a^3 k^2) \text{ Np/m.}\end{aligned}\quad (3.96)$$

TM Modes

TM modes are characterized by fields with $H_z = 0$, while E_z must satisfy the reduced wave equation (3.25):

$$\left(\frac{\partial^2}{\partial x^2} + \frac{\partial^2}{\partial y^2} + k_c^2 \right) e_z(x, y) = 0, \quad (3.97)$$

with $E_z(x, y, z) = e_z(x, y) e^{-j\beta z}$ and $k_c^2 = k^2 - \beta^2$. Equation (3.97) can be solved by the separation-of-variables procedure that was used for TE modes. The general solution is

$$e_z(x, y) = (A \cos k_x x + B \sin k_x x)(C \cos k_y y + D \sin k_y y). \quad (3.98)$$

The boundary conditions can be applied directly to e_z :

$$e_z(x, y) = 0, \quad \text{at } x = 0, a, \quad (3.99a)$$

$$e_z(x, y) = 0, \quad \text{at } y = 0, b. \quad (3.99b)$$

We will see that satisfaction of these conditions on e_z will lead to satisfaction of the boundary conditions by e_x and e_y .

Applying (3.99a) to (3.98) shows that $A = 0$ and $k_x = m\pi/a$ for $m = 1, 2, 3, \dots$. Similarly, applying (3.99b) to (3.98) shows that $C = 0$ and $k_y = n\pi/b$ for $n = 1, 2, 3, \dots$. The solution for E_z then reduces to

$$E_z(x, y, z) = B_{mn} \sin \frac{m\pi x}{a} \sin \frac{n\pi y}{b} e^{-j\beta z}, \quad (3.100)$$

where B_{mn} is an arbitrary amplitude constant.

The transverse field components for the TM_{mn} mode can be computed from (3.23) and (3.100) as

$$E_x = \frac{-j\beta m\pi}{a k_c^2} B_{mn} \cos \frac{m\pi x}{a} \sin \frac{n\pi y}{b} e^{-j\beta z}, \quad (3.101a)$$

$$E_y = \frac{-j\beta n\pi}{b k_c^2} B_{mn} \sin \frac{m\pi x}{a} \cos \frac{n\pi y}{b} e^{-j\beta z}, \quad (3.101b)$$

$$H_x = \frac{j\omega \epsilon n\pi}{b k_c^2} B_{mn} \sin \frac{m\pi x}{a} \cos \frac{n\pi y}{b} e^{-j\beta z}, \quad (3.101c)$$

$$H_y = \frac{-j\omega \epsilon m\pi}{a k_c^2} B_{mn} \cos \frac{m\pi x}{a} \sin \frac{n\pi y}{b} e^{-j\beta z}. \quad (3.101d)$$

As for the TE modes, the propagation constant is

$$\beta = \sqrt{k^2 - k_c^2} = \sqrt{k^2 - \left(\frac{m\pi}{a}\right)^2 - \left(\frac{n\pi}{b}\right)^2} \quad (3.102)$$

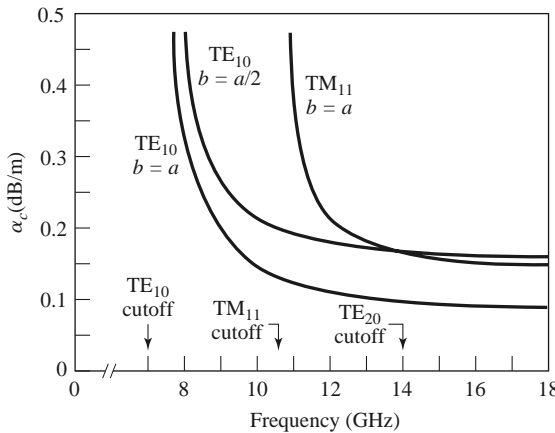


FIGURE 3.8 Attenuation of various modes in a rectangular brass waveguide with $a = 2.0$ cm.

and is real for propagating modes and imaginary for cutoff modes. The cutoff frequencies for the TM_{mn} modes are also the same as those of the TE_{mn} modes, as given in (3.84). The guide wavelength and phase velocity for TM modes are also the same as those for TE modes.

Observe that the field expressions for \bar{E} and \bar{H} in (3.101) are identically zero if either m or n is zero. Thus there is no TM_{00} , TM_{01} , or TM_{10} mode, and the lowest order TM mode to propagate (lowest f_c) is the TM_{11} mode, having a cutoff frequency of

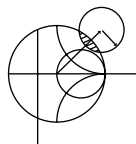
$$f_{c11} = \frac{1}{2\pi\sqrt{\mu\epsilon}} \sqrt{\left(\frac{\pi}{a}\right)^2 + \left(\frac{\pi}{b}\right)^2}, \quad (3.103)$$

which is seen to be larger than f_{c10} , the cutoff frequency of the TE_{10} mode.

The wave impedance relating the transverse electric and magnetic fields for TM modes is, from (3.26),

$$Z_{\text{TM}} = \frac{E_x}{H_y} = \frac{-E_y}{H_x} = \frac{\beta\eta}{k}. \quad (3.104)$$

Attenuation due to dielectric loss is computed in the same way as for TE modes, with the same result. The calculation of attenuation due to conductor loss is left as a problem; Figure 3.8 shows attenuation versus frequency for some TE and TM modes in a rectangular waveguide. Table 3.2 summarizes results for TE and TM wave propagation in rectangular waveguides, and Figure 3.9 shows the field lines for several of the lowest order TE and TM modes.



EXAMPLE 3.1 CHARACTERISTICS OF A RECTANGULAR WAVEGUIDE

Consider a length of Teflon-filled, copper K-band rectangular waveguide having dimensions $a = 1.07$ cm and $b = 0.43$ cm. Find the cutoff frequencies of the first five propagating modes. If the operating frequency is 15 GHz, find the attenuation due to dielectric and conductor losses.

TABLE 3.2 Summary of Results for Rectangular Waveguide

Quantity	TE _{mn} Mode	TM _{mn} Mode
k	$\omega\sqrt{\mu\epsilon}$	$\omega\sqrt{\mu\epsilon}$
k_c	$\sqrt{(m\pi/a)^2 + (n\pi/b)^2}$	$\sqrt{(m\pi/a)^2 + (n\pi/b)^2}$
β	$\sqrt{k^2 - k_c^2}$	$\sqrt{k^2 - k_c^2}$
λ_c	$\frac{2\pi}{k_c}$	$\frac{2\pi}{k_c}$
λ_g	$\frac{2\pi}{\beta}$	$\frac{2\pi}{\beta}$
v_p	$\frac{\omega}{\beta}$	$\frac{\omega}{\beta}$
α_d	$\frac{k^2 \tan \delta}{2\beta}$	$\frac{k^2 \tan \delta}{2\beta}$
E_z	0	$B \sin \frac{m\pi x}{a} \sin \frac{n\pi y}{b} e^{-j\beta z}$
H_z	$A \cos \frac{m\pi x}{a} \cos \frac{n\pi y}{b} e^{-j\beta z}$	0
E_x	$\frac{j\omega\mu n\pi}{k_c^2 b} A \cos \frac{m\pi x}{a} \sin \frac{n\pi y}{b} e^{-j\beta z}$	$\frac{-j\beta m\pi}{k_c^2 a} B \cos \frac{m\pi x}{a} \sin \frac{n\pi y}{b} e^{-j\beta z}$
E_y	$\frac{-j\omega\mu m\pi}{k_c^2 a} A \sin \frac{m\pi x}{a} \cos \frac{n\pi y}{b} e^{-j\beta z}$	$\frac{-j\beta n\pi}{k_c^2 b} B \sin \frac{m\pi x}{a} \cos \frac{n\pi y}{b} e^{-j\beta z}$
H_x	$\frac{j\beta m\pi}{k_c^2 a} A \sin \frac{m\pi x}{a} \cos \frac{n\pi y}{b} e^{-j\beta z}$	$\frac{j\omega\epsilon n\pi}{k_c^2 b} B \sin \frac{m\pi x}{a} \cos \frac{n\pi y}{b} e^{-j\beta z}$
H_y	$\frac{j\beta n\pi}{k_c^2 b} A \cos \frac{m\pi x}{a} \sin \frac{n\pi y}{b} e^{-j\beta z}$	$\frac{-j\omega\epsilon m\pi}{k_c^2 a} B \cos \frac{m\pi x}{a} \sin \frac{n\pi y}{b} e^{-j\beta z}$
Z	$Z_{\text{TE}} = \frac{k\eta}{\beta}$	$Z_{\text{TM}} = \frac{\beta\eta}{k}$

Solution

From Appendix G, for Teflon, $\epsilon_r = 2.08$ and $\tan \delta = 0.0004$. From (3.84) the cutoff frequencies are given by

$$f_{c_{mn}} = \frac{c}{2\pi\sqrt{\epsilon_r}} \sqrt{\left(\frac{m\pi}{a}\right)^2 + \left(\frac{n\pi}{b}\right)^2}.$$

Computing f_c for the first few values of m and n gives the following results:

Mode	m	n	f_c (GHz)
TE	1	0	9.72
TE	2	0	19.44
TE	0	1	24.19
TE, TM	1	1	26.07
TE, TM	2	1	31.03

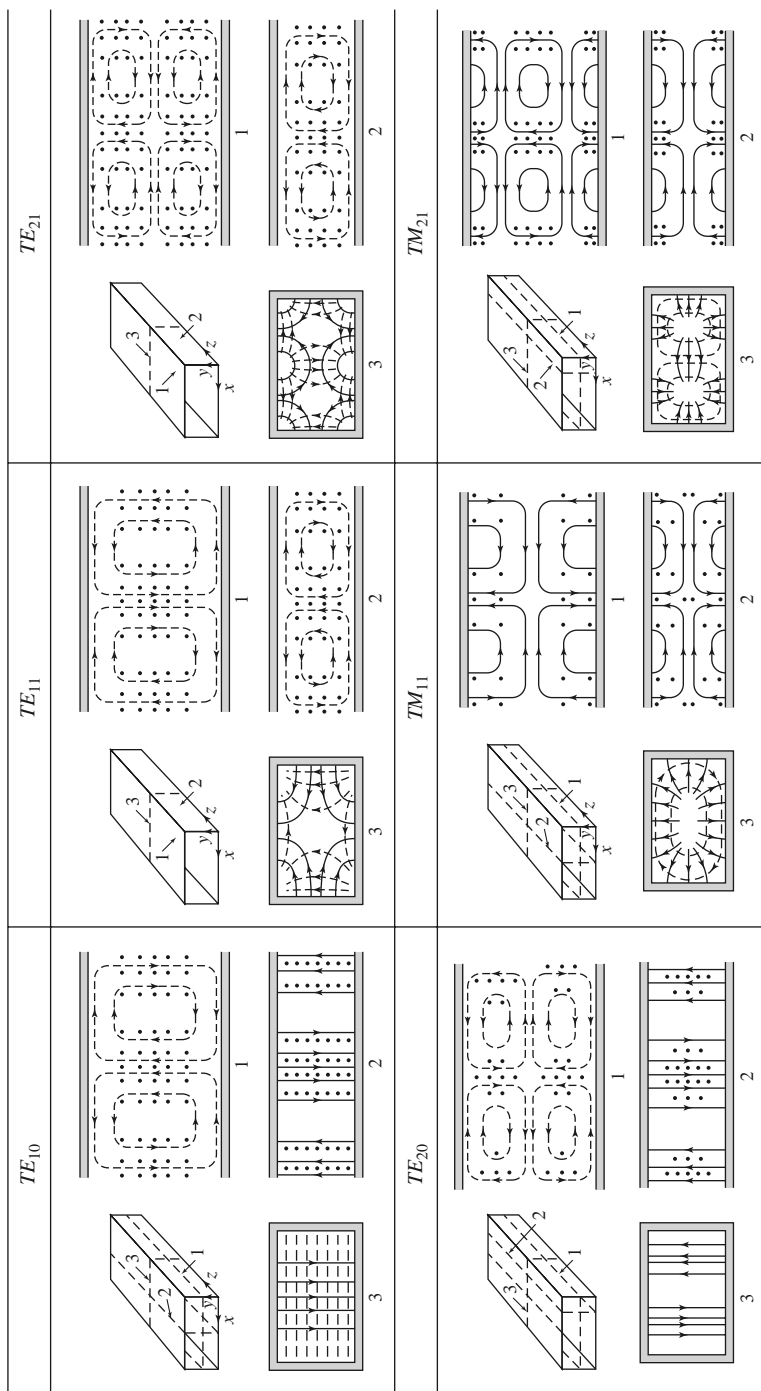


FIGURE 3.9 Field lines for some of the lower order modes of a rectangular waveguide.

Reprinted with permission from S. Ramo, J. R. Whinnery, and T. Van Duzer, *Fields and Waves in Communication Electronics*. Copyright © 1965 by John Wiley & Sons, Inc. Table 8.02.

Thus the TE_{10} , TE_{20} , TE_{01} , TE_{11} , and TM_{11} modes will be the first five modes to propagate.

At 15 GHz, $k = 453.1 \text{ m}^{-1}$, and the propagation constant for the TE_{10} mode is

$$\beta = \sqrt{\left(\frac{2\pi f \sqrt{\epsilon_r}}{c}\right)^2 - \left(\frac{\pi}{a}\right)^2} = \sqrt{k^2 - \left(\frac{\pi}{a}\right)^2} = 345.1 \text{ m}^{-1}.$$

From (3.29), the attenuation due to dielectric loss is

$$\alpha_d = \frac{k^2 \tan \delta}{2\beta} = 0.119 \text{ Np/m} = 1.03 \text{ dB/m.}$$

The surface resistivity of the copper walls is ($\sigma = 5.8 \times 10^7 \text{ S/m}$)

$$R_s = \sqrt{\frac{\omega \mu_0}{2\sigma}} = 0.032 \Omega,$$

and the attenuation due to conductor loss, from (3.96), is

$$\alpha_c = \frac{R_s}{a^3 b \beta k \eta} (2b\pi^2 + a^3 k^2) = 0.050 \text{ Np/m} = 0.434 \text{ dB/m.}$$

■

TE _{$m0$} Modes of a Partially Loaded Waveguide

The above results apply to an empty waveguide as well as one filled with a homogeneous dielectric or magnetic material, but in some cases of practical interest (such as impedance matching or phase-shifting sections) a waveguide is used with a partial dielectric filling. In this case an additional set of boundary conditions are introduced at the material interface, necessitating a new analysis. To illustrate the technique we will consider the TE _{$m0$} modes of a rectangular waveguide that is partially filled with a dielectric slab, as shown in Figure 3.10. The analysis still follows the basic procedure outlined at the end of Section 3.1.

Since the geometry is uniform in the y direction and $n = 0$, the TE _{$m0$} modes have no y dependence. Then the wave equation of (3.21) for h_z can be written separately for the dielectric and air regions as

$$\left(\frac{\partial^2}{\partial x^2} + k_d^2\right)h_z = 0, \quad \text{for } 0 \leq x \leq t, \quad (3.105a)$$

$$\left(\frac{\partial^2}{\partial x^2} + k_a^2\right)h_z = 0, \quad \text{for } t \leq x \leq a, \quad (3.105b)$$

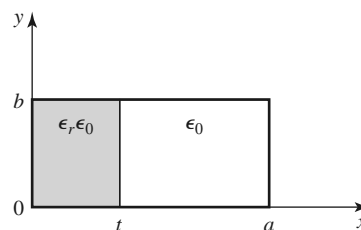


FIGURE 3.10 Geometry of a partially loaded rectangular waveguide.

where k_d and k_a are the cutoff wave numbers for the dielectric and air regions, defined as follows:

$$\beta = \sqrt{\epsilon_r k_0^2 - k_d^2}, \quad (3.106a)$$

$$\beta = \sqrt{k_0^2 - k_a^2}. \quad (3.106b)$$

These relations incorporate the fact that the propagation constant, β , must be the same in both regions to ensure phase matching (see Section 1.8) of the fields along the interface at $x = t$. The solutions to (3.105) can be written as

$$h_z = \begin{cases} A \cos k_d x + B \sin k_d x & \text{for } 0 \leq x \leq t \\ C \cos k_a (a - x) + D \sin k_a (a - x) & \text{for } t \leq x \leq a, \end{cases} \quad (3.107)$$

where the form of the solution for $t < x < a$ was chosen to simplify the evaluation of boundary conditions at $x = a$.

We need \hat{y} and \hat{z} electric and magnetic field components to apply the boundary conditions at $x = 0$, t , and a . $E_z = 0$ for TE modes, and $H_y = 0$ since $\partial/\partial y = 0$. E_y is found from (3.19d) as

$$e_y = \begin{cases} \frac{j\omega\mu_0}{k_d} (-A \sin k_d x + B \cos k_d x) & \text{for } 0 \leq x \leq t \\ \frac{j\omega\mu_0}{k_a} [C \sin k_a (a - x) - D \cos k_a (a - x)] & \text{for } t \leq x \leq a. \end{cases} \quad (3.108)$$

To satisfy the boundary conditions that $E_y = 0$ at $x = 0$ and $x = a$ requires that $B = D = 0$. We next enforce continuity of tangential fields (E_y , H_z) at $x = t$. Equations (3.107) and (3.108) then give the following:

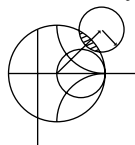
$$\begin{aligned} \frac{-A}{k_d} \sin k_d t &= \frac{C}{k_a} \sin k_a (a - t), \\ A \cos k_d t &= C \cos k_a (a - t). \end{aligned}$$

Because this is a homogeneous set of equations, the determinant must vanish in order to have a nontrivial solution. Thus,

$$k_a \tan k_d t + k_d \tan k_a (a - t) = 0. \quad (3.109)$$

Using (3.106) allows k_a and k_d to be expressed in terms of β , so (3.109) can be solved numerically for β . There is an infinite number of solutions to (3.109), corresponding to the propagation constants of the TE_{m0} modes.

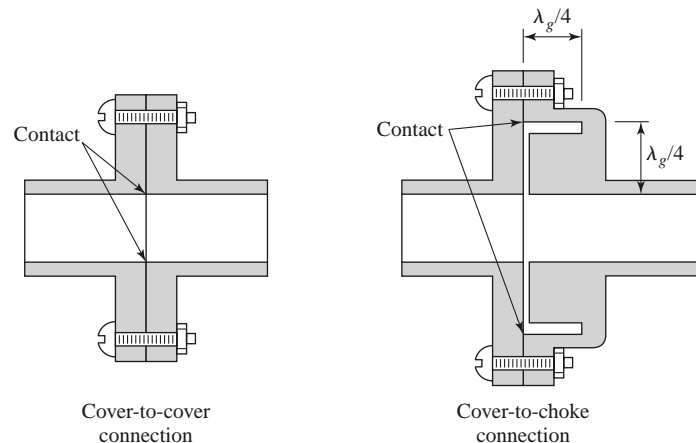
This technique can be applied to many other waveguide geometries involving dielectric or magnetic material inhomogeneities, such as the surface waveguide of Section 3.6 or the ferrite-loaded waveguide of Section 9.3. In some cases, however, it will be impossible to satisfy all the necessary boundary conditions with only TE- or TM-type modes, and a hybrid combination of both types of modes may be required.



POINT OF INTEREST: Waveguide Flanges

There are two commonly used waveguide flanges: the cover flange and the choke flange. As shown in the accompanying figure, two waveguides with cover-type flanges can be bolted together to form a contacting joint. To avoid reflections and resistive loss at this joint it is necessary that the contacting surfaces be smooth, clean, and square because RF currents must flow across this discontinuity. In high-power applications voltage breakdown may occur at an imperfect junction. Otherwise, the simplicity of the cover-to-cover connection makes it preferable for general use. The SWR from such a joint is typically less than 1.03.

An alternative waveguide connection uses a cover flange against a choke flange, as shown in the figure. The choke flange is machined to form an effective radial transmission line in the narrow gap between the two flanges; this line is approximately $\lambda_g/4$ in length between the guide and the point of contact for the two flanges. Another $\lambda_g/4$ line is formed by a circular axial groove in the choke flange. Then the short circuit at the right-hand end of this groove is transformed into an open circuit at the contact point of the flanges. Any resistance in this contact is in series with an infinite (or very high) impedance and thus has little effect. This high impedance is transformed back into a short circuit (or very low impedance) at the edges of the waveguides to provide an effective low-resistance path for current flow across the joint. Because there is a negligible voltage drop across the ohmic contact between the flanges, voltage breakdown is avoided. Thus, the cover-to-choke connection can be useful for high-power applications. The SWR for this joint is typically less than 1.05 but is more frequency dependent than that of the cover-to-cover joint.



Reference: C. G. Montgomery, R. H. Dicke, and E. M. Purcell, *Principles of Microwave Circuits*, McGraw-Hill, New York, 1948.

3.4 CIRCULAR WAVEGUIDE

A hollow, round metal pipe also supports TE and TM waveguide modes. Figure 3.11 shows the geometry of such a circular waveguide, with inner radius a . Because cylindrical geometry is involved, it is appropriate to employ cylindrical coordinates. As in the rectangular

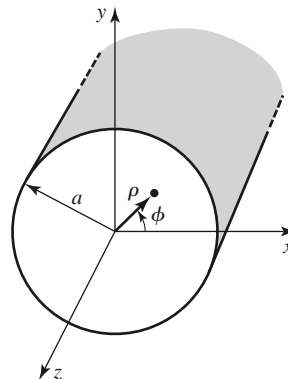


FIGURE 3.11 Geometry of a circular waveguide.

coordinate case, the transverse fields in cylindrical coordinates can be derived from E_z or H_z field components for TM and TE modes, respectively. Paralleling the development of Section 3.1, we can derive the cylindrical components of the transverse fields from the longitudinal components as

$$E_\rho = \frac{-j}{k_c^2} \left(\beta \frac{\partial E_z}{\partial \rho} + \frac{\omega \mu}{\rho} \frac{\partial H_z}{\partial \phi} \right), \quad (3.110a)$$

$$E_\phi = \frac{-j}{k_c^2} \left(\frac{\beta}{\rho} \frac{\partial E_z}{\partial \phi} - \omega \mu \frac{\partial H_z}{\partial \rho} \right), \quad (3.110b)$$

$$H_\rho = \frac{j}{k_c^2} \left(\frac{\omega \epsilon}{\rho} \frac{\partial E_z}{\partial \phi} - \beta \frac{\partial H_z}{\partial \rho} \right), \quad (3.110c)$$

$$H_\phi = \frac{-j}{k_c^2} \left(\omega \epsilon \frac{\partial E_z}{\partial \rho} + \frac{\beta}{\rho} \frac{\partial H_z}{\partial \phi} \right), \quad (3.110d)$$

where $k_c^2 = k^2 - \beta^2$, and $e^{-j\beta z}$ propagation has been assumed. For $e^{+j\beta z}$ propagation, replace β with $-\beta$ in all expressions.

TE Modes

For TE modes, $E_z = 0$, and H_z is a solution to the wave equation,

$$\nabla^2 H_z + k^2 H_z = 0. \quad (3.111)$$

If $H_z(\rho, \phi, z) = h_z(\rho, \phi)e^{-j\beta z}$, (3.111) can be expressed in cylindrical coordinates as

$$\left(\frac{\partial^2}{\partial \rho^2} + \frac{1}{\rho} \frac{\partial}{\partial \rho} + \frac{1}{\rho^2} \frac{\partial^2}{\partial \phi^2} + k_c^2 \right) h_z(\rho, \phi) = 0. \quad (3.112)$$

As before, we apply the method of separation of variables. Thus, let

$$h_z(\rho, \phi) = R(\rho)P(\phi), \quad (3.113)$$

and substitute into (3.112) to obtain

$$\frac{1}{R} \frac{d^2 R}{d \rho^2} + \frac{1}{\rho R} \frac{d R}{d \rho} + \frac{1}{\rho^2 P} \frac{d^2 P}{d \phi^2} + k_c^2 = 0,$$

or

$$\frac{\rho^2}{R} \frac{d^2 R}{d \rho^2} + \frac{\rho}{R} \frac{d R}{d \rho} + \rho^2 k_c^2 = \frac{-1}{P} \frac{d^2 P}{d \phi^2}. \quad (3.114)$$

The left side of this equation depends only on ρ (not ϕ), while the right side depends only on ϕ . Thus, each side must be equal to a constant, which we will call k_ϕ^2 . Then,

$$\frac{-1}{P} \frac{d^2 P}{d \phi^2} = k_\phi^2,$$

or

$$\frac{d^2 P}{d \phi^2} + k_\phi^2 P = 0. \quad (3.115)$$

In addition,

$$\rho^2 \frac{d^2 R}{d\rho^2} + \rho \frac{dR}{d\rho} + (\rho^2 k_c^2 - k_\phi^2) R = 0. \quad (3.116)$$

The general solution to (3.115) is

$$P(\phi) = A \sin k_\phi \phi + B \cos k_\phi \phi. \quad (3.117)$$

Because the solution to h_z must be periodic in ϕ [i.e., $h_z(\rho, \phi) = h_z(\rho, \phi \pm 2m\pi)$], k_ϕ must be an integer, n . Thus (3.117) becomes

$$P(\phi) = A \sin n\phi + B \cos n\phi, \quad (3.118)$$

and (3.116) becomes

$$\rho^2 \frac{d^2 R}{d\rho^2} + \rho \frac{dR}{d\rho} + (\rho^2 k_c^2 - n^2) R = 0, \quad (3.119)$$

which is recognized as Bessel's differential equation. The solution is

$$R(\rho) = C J_n(k_c \rho) + D Y_n(k_c \rho), \quad (3.120)$$

where $J_n(x)$ and $Y_n(x)$ are the Bessel functions of first and second kinds, respectively. Because $Y_n(k_c \rho)$ becomes infinite at $\rho = 0$, this term is physically unacceptable for a circular waveguide, so $D = 0$. The solution for h_z can then be simplified to

$$h_z(\rho, \phi) = (A \sin n\phi + B \cos n\phi) J_n(k_c \rho), \quad (3.121)$$

where the constant C of (3.120) has been absorbed into the constants A and B of (3.121). We must still determine the cutoff wave number k_c , which we can do by enforcing the boundary condition that $E_{\tan} = 0$ on the waveguide wall. Because $E_z = 0$, we must have that

$$E_\phi(\rho, \phi) = 0 \quad \text{at } \rho = a. \quad (3.122)$$

From (3.110b), we find E_ϕ from H_z as

$$E_\phi(\rho, \phi, z) = \frac{j\omega\mu}{k_c} (A \sin n\phi + B \cos n\phi) J'_n(k_c \rho) e^{-j\beta z}, \quad (3.123)$$

where the notation $J'_n(k_c \rho)$ refers to the derivative of J_n with respect to its argument. For E_ϕ to vanish at $\rho = a$, we must have

$$J'_n(k_c a) = 0. \quad (3.124)$$

If the roots of $J'_n(x)$ are defined as p'_{nm} , so that $J'_n(p'_{nm}) = 0$, where p'_{nm} is the m th root of J'_n , then k_c must have the value

$$k_{c_{nm}} = \frac{p'_{nm}}{a}. \quad (3.125)$$

Values of p'_{nm} are given in mathematical tables; the first few values are listed in Table 3.3.

TABLE 3.3 Values of p'_{nm} for TE Modes of a Circular Waveguide

n	p'_{n1}	p'_{n2}	p'_{n3}
0	3.832	7.016	10.174
1	1.841	5.331	8.536
2	3.054	6.706	9.970

The TE_{nm} modes are thus defined by the cutoff wave number $k_{c_{nm}} = p'_{nm}/a$, where n refers to the number of circumferential (ϕ) variations and m refers to the number of radial (ρ) variations. The propagation constant of the TE_{nm} mode is

$$\beta_{nm} = \sqrt{k^2 - k_c^2} = \sqrt{k^2 - \left(\frac{p'_{nm}}{a}\right)^2}, \quad (3.126)$$

with a cutoff frequency of

$$f_{c_{nm}} = \frac{k_c}{2\pi\sqrt{\mu\epsilon}} = \frac{p'_{nm}}{2\pi a\sqrt{\mu\epsilon}}. \quad (3.127)$$

The first TE mode to propagate is the mode with the smallest p'_{nm} , which from Table 3.3 is seen to be the TE₁₁ mode. This mode is therefore the dominant circular waveguide mode and the one most frequently used. Because $m \geq 1$, there is no TE₁₀ mode, but there is a TE₀₁ mode.

The transverse field components are, from (3.110) and (3.121),

$$E_\rho = \frac{-j\omega\mu n}{k_c^2 \rho} (A \cos n\phi - B \sin n\phi) J_n(k_c \rho) e^{-j\beta z}, \quad (3.128a)$$

$$E_\phi = \frac{j\omega\mu}{k_c} (A \sin n\phi + B \cos n\phi) J'_n(k_c \rho) e^{-j\beta z}, \quad (3.128b)$$

$$H_\rho = \frac{-j\beta}{k_c} (A \sin n\phi + B \cos n\phi) J'_n(k_c \rho) e^{-j\beta z}, \quad (3.128c)$$

$$H_\phi = \frac{-j\beta n}{k_c^2 \rho} (A \cos n\phi - B \sin n\phi) J_n(k_c \rho) e^{-j\beta z}. \quad (3.128d)$$

The wave impedance is

$$Z_{\text{TE}} = \frac{E_\rho}{H_\phi} = \frac{-E_\phi}{H_\rho} = \frac{\eta k}{\beta}. \quad (3.129)$$

In the above solutions there are two remaining arbitrary amplitude constants, A and B . These constants control the amplitude of the $\sin n\phi$ and $\cos n\phi$ terms, which are independent. That is, because of the azimuthal symmetry of the circular waveguide, both the $\sin n\phi$ and $\cos n\phi$ terms represent valid solutions, and both may be present in a specific problem. The actual amplitudes of these terms will depend on the excitation of the waveguide. From a different viewpoint, the coordinate system can be rotated about the z -axis to obtain an h_z with either $A = 0$ or $B = 0$.

Now consider the dominant TE₁₁ mode with an excitation such that $B = 0$. The fields can be written as

$$H_z = A \sin \phi J_1(k_c \rho) e^{-j\beta z}, \quad (3.130a)$$

$$E_\rho = \frac{-j\omega\mu}{k_c^2 \rho} A \cos \phi J_1(k_c \rho) e^{-j\beta z}, \quad (3.130b)$$

$$E_\phi = \frac{j\omega\mu}{k_c} A \sin \phi J'_1(k_c \rho) e^{-j\beta z}, \quad (3.130c)$$

$$H_\rho = \frac{-j\beta}{k_c} A \sin \phi J'_1(k_c \rho) e^{-j\beta z}, \quad (3.130d)$$

$$H_\phi = \frac{-j\beta}{k_c^2 \rho} A \cos \phi J_1(k_c \rho) e^{-j\beta z}, \quad (3.130e)$$

$$E_z = 0. \quad (3.130f)$$

The power flow down the guide can be computed as

$$\begin{aligned}
P_o &= \frac{1}{2} \operatorname{Re} \int_{\rho=0}^a \int_{\phi=0}^{2\pi} \bar{E} \times \bar{H}^* \cdot \hat{z} \rho d\phi d\rho \\
&= \frac{1}{2} \operatorname{Re} \int_{\rho=0}^a \int_{\phi=0}^{2\pi} (E_\rho H_\phi^* - E_\phi H_\rho^*) \rho d\phi d\rho \\
&= \frac{\omega\mu|A|^2 \operatorname{Re}(\beta)}{2k_c^4} \int_{\rho=0}^a \int_{\phi=0}^{2\pi} \left[\frac{1}{\rho^2} \cos^2 \phi J_1^2(k_c \rho) + k_c^2 \sin^2 \phi J_1'^2(k_c \rho) \right] \rho d\phi d\rho \\
&= \frac{\pi\omega\mu|A|^2 \operatorname{Re}(\beta)}{2k_c^4} \int_{\rho=0}^a \left[\frac{1}{\rho} J_1^2(k_c \rho) + \rho k_c^2 J_1'^2(k_c \rho) \right] d\rho \\
&= \frac{\pi\omega\mu|A|^2 \operatorname{Re}(\beta)}{4k_c^4} (p_{11}'^2 - 1) J_1^2(k_c a), \tag{3.131}
\end{aligned}$$

which is seen to be nonzero only when β is real, corresponding to a propagating mode. (The required integral for this result is given in Appendix C.)

Attenuation due to dielectric loss is given by (3.29). The attenuation due to a lossy waveguide conductor can be found by computing the power loss per unit length of guide:

$$\begin{aligned}
P_\ell &= \frac{R_s}{2} \int_{\phi=0}^{2\pi} |\bar{J}_s|^2 a d\phi \\
&= \frac{R_s}{2} \int_{\phi=0}^{2\pi} (|H_\phi|^2 + |H_z|^2) a d\phi \\
&= \frac{|A|^2 R_s}{2} \int_{\phi=0}^{2\pi} \left(\frac{\beta^2}{k_c^4 a^2} \cos^2 \phi + \sin^2 \phi \right) J_1^2(k_c a) a d\phi \\
&= \frac{\pi |A|^2 R_s a}{2} \left(1 + \frac{\beta^2}{k_c^4 a^2} \right) J_1^2(k_c a). \tag{3.132}
\end{aligned}$$

The attenuation constant is then

$$\begin{aligned}
\alpha_c &= \frac{P_\ell}{2P_o} = \frac{R_s (k_c^4 a^2 + \beta^2)}{\eta k \beta a (p_{11}'^2 - 1)} \\
&= \frac{R_s}{a k \eta \beta} \left(k_c^2 + \frac{k^2}{p_{11}'^2 - 1} \right) \text{Np/m.} \tag{3.133}
\end{aligned}$$

TM Modes

For the TM modes of the circular waveguide, we must solve for E_z from the wave equation in cylindrical coordinates:

$$\left(\frac{\partial^2}{\partial \rho^2} + \frac{1}{\rho} \frac{\partial}{\partial \rho} + \frac{1}{\rho^2} \frac{\partial^2}{\partial \phi^2} + k_c^2 \right) e_z = 0, \tag{3.134}$$

where $E_z(\rho, \phi, z) = e_z(\rho, \phi) e^{-j\beta z}$, and $k_c^2 = k^2 - \beta^2$. Because this equation is identical to (3.107), the general solutions are the same. Thus, from (3.121),

$$e_z(\rho, \phi) = (A \sin n\phi + B \cos n\phi) J_n(k_c \rho). \tag{3.135}$$

TABLE 3.4 Values of p_{nm} for TM Modes of a Circular Waveguide

n	p_{n1}	p_{n2}	p_{n3}
0	2.405	5.520	8.654
1	3.832	7.016	10.174
2	5.135	8.417	11.620

The difference between the TE solution and the present solution is that the boundary conditions can now be applied directly to e_z of (3.135) since

$$E_z(\rho, \phi) = 0 \quad \text{at } \rho = a. \quad (3.136)$$

Thus, we must have

$$J_n(k_c a) = 0, \quad (3.137)$$

or

$$k_c = p_{nm}/a, \quad (3.138)$$

where p_{nm} is the m th root of $J_n(x)$, that is, $J_n(p_{nm}) = 0$. Values of p_{nm} are given in mathematical tables; the first few values are listed in Table 3.4.

The propagation constant of the TM_{nm} mode is

$$\beta_{nm} = \sqrt{k^2 - k_c^2} = \sqrt{k^2 - (p_{nm}/a)^2}, \quad (3.139)$$

and the cutoff frequency is

$$f_{c_{nm}} = \frac{k_c}{2\pi\sqrt{\mu\epsilon}} = \frac{p_{nm}}{2\pi a\sqrt{\mu\epsilon}}. \quad (3.140)$$

Thus, the first TM mode to propagate is the TM_{01} mode, with $p_{01} = 2.405$. Because this is greater than $p'_{11} = 1.841$ for the lowest order TE_{11} mode, the TE_{11} mode is the dominant mode of the circular waveguide. As with the TE modes, $m \geq 1$, so there is no TM_{10} mode.

From (3.110), the transverse fields can be derived as

$$E_\rho = \frac{-j\beta}{k_c} (A \sin n\phi + B \cos n\phi) J'_n(k_c \rho) e^{-j\beta z}, \quad (3.141a)$$

$$E_\phi = \frac{-j\beta n}{k_c^2 \rho} (A \cos n\phi - B \sin n\phi) J_n(k_c \rho) e^{-j\beta z}, \quad (3.141b)$$

$$H_\rho = \frac{j\omega\epsilon n}{k_c^2 \rho} (A \cos n\phi - B \sin n\phi) J_n(k_c \rho) e^{-j\beta z}, \quad (3.141c)$$

$$H_\phi = \frac{-j\omega\epsilon}{k_c} (A \sin n\phi + B \cos n\phi) J'_n(k_c \rho) e^{-j\beta z}. \quad (3.141d)$$

The wave impedance is

$$Z_{\text{TM}} = \frac{E_\rho}{H_\phi} = \frac{-E_\phi}{H_\rho} = \frac{\eta\beta}{k}. \quad (3.142)$$

Calculation of the attenuation for TM modes is left as a problem. Figure 3.12 shows the attenuation due to conductor loss versus frequency for various modes of a circular waveguide. Observe that the attenuation of the TE_{01} mode decreases to a very small value with

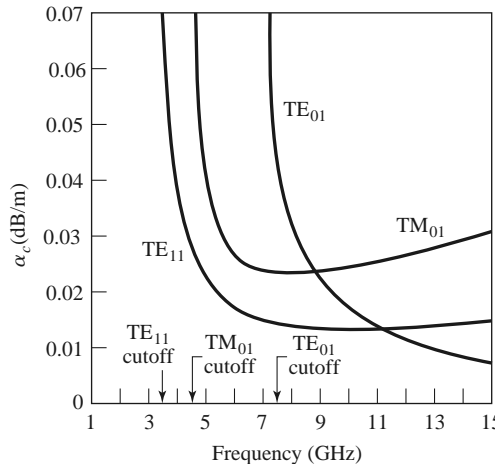


FIGURE 3.12 Attenuation of various modes in a circular copper waveguide with $a = 2.54$ cm.

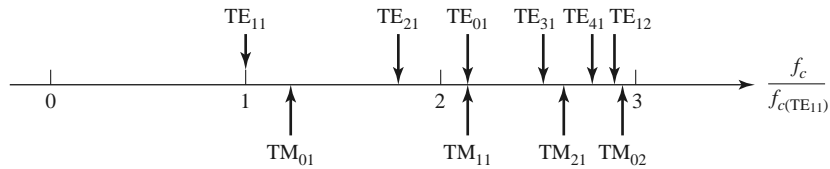
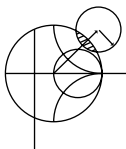


FIGURE 3.13 Cutoff frequencies of the first few TE and TM modes of a circular waveguide relative to the cutoff frequency of the dominant TE_{11} mode.

increasing frequency. This property makes the TE_{01} mode of interest for low-loss transmission over long distances. Unfortunately, this mode is not the dominant mode of the circular waveguide, so in practice power can be lost from the TE_{01} mode to lower order propagating modes.

Figure 3.13 shows the relative cutoff frequencies of the TE and TM modes, and Table 3.5 summarizes results for wave propagation in circular waveguide. Field lines for some of the lowest order TE and TM modes are shown in Figure 3.14.



EXAMPLE 3.2 CHARACTERISTICS OF A CIRCULAR WAVEGUIDE

Find the cutoff frequencies of the first two propagating modes of a Teflon-filled circular waveguide with $a = 0.5$ cm. If the interior of the guide is gold plated, calculate the overall loss in dB for a 30 cm length operating at 14 GHz.

Solution

From Figure 3.13, the first two propagating modes of a circular waveguide are the TE_{11} and TM_{01} modes. The cutoff frequencies can be found using (3.127) and (3.140):

$$TE_{11}: \quad f_c = \frac{p'_{11}c}{2\pi a\sqrt{\epsilon_r}} = \frac{1.841(3 \times 10^8)}{2\pi(0.005)\sqrt{2.08}} = 12.19 \text{ GHz},$$

$$TM_{01}: \quad f_c = \frac{p_{01}c}{2\pi a\sqrt{\epsilon_r}} = \frac{2.405(3 \times 10^8)}{2\pi(0.005)\sqrt{2.08}} = 15.92 \text{ GHz}.$$

TABLE 3.5 Summary of Results for Circular Waveguide

Quantity	TE _{nm} Mode	TM _{nm} Mode
k	$\omega\sqrt{\mu\epsilon}$	$\omega\sqrt{\mu\epsilon}$
k_c	$\frac{p'_{nm}}{a}$	$\frac{p_{nm}}{a}$
β	$\sqrt{k^2 - k_c^2}$	$\sqrt{k^2 - k_c^2}$
λ_c	$\frac{2\pi}{k_c}$	$\frac{2\pi}{k_c}$
λ_g	$\frac{2\pi}{\beta}$	$\frac{2\pi}{\beta}$
v_p	$\frac{\omega}{\beta}$	$\frac{\omega}{\beta}$
α_d	$\frac{k^2 \tan \delta}{2\beta}$	$\frac{k^2 \tan \delta}{2\beta}$
E_z	0	$(A \sin n\phi + B \cos n\phi) J_n(k_c \rho) e^{-j\beta z}$
H_z	$(A \sin n\phi + B \cos n\phi) J_n(k_c \rho) e^{-j\beta z}$	0
E_ρ	$\frac{-j\omega\mu n}{k_c^2 \rho} (A \cos n\phi - B \sin n\phi) J_n(k_c \rho) e^{-j\beta z}$	$\frac{-j\beta}{k_c} (A \sin n\phi + B \cos n\phi) J'_n(k_c \rho) e^{-j\beta z}$
E_ϕ	$\frac{j\omega\mu}{k_c} (A \sin n\phi + B \cos n\phi) J'_n(k_c \rho) e^{-j\beta z}$	$\frac{-j\beta n}{k_c^2 \rho} (A \cos n\phi - B \sin n\phi) J_n(k_c \rho) e^{-j\beta z}$
H_ρ	$\frac{-j\beta}{k_c} (A \sin n\phi + B \cos n\phi) J'_n(k_c \rho) e^{-j\beta z}$	$\frac{j\omega\epsilon n}{k_c^2 \rho} (A \cos n\phi - B \sin n\phi) J_n(k_c \rho) e^{-j\beta z}$
H_ϕ	$\frac{-j\beta n}{k_c^2 \rho} (A \cos n\phi - B \sin n\phi) J_n(k_c \rho) e^{-j\beta z}$	$\frac{-j\omega\epsilon}{k_c} (A \sin n\phi + B \cos n\phi) J'_n(k_c \rho) e^{-j\beta z}$
Z	$Z_{\text{TE}} = \frac{k\eta}{\beta}$	$Z_{\text{TM}} = \frac{\beta\eta}{k}$

So only the TE₁₁ mode is propagating at 14 GHz. The wave number is

$$k = \frac{2\pi f \sqrt{\epsilon_r}}{c} = \frac{2\pi (14 \times 10^9) \sqrt{2.08}}{3 \times 10^8} = 422.9 \text{ m}^{-1},$$

and the propagation constant of the TE₁₁ mode is

$$\beta = \sqrt{k^2 - \left(\frac{p'_{11}}{a}\right)^2} = \sqrt{(422.9)^2 - \left(\frac{1.841}{0.005}\right)^2} = 208.0 \text{ m}^{-1}.$$

The attenuation due to dielectric loss is calculated from (3.29) as

$$\alpha_d = \frac{k^2 \tan \delta}{2\beta} = \frac{(422.9)^2 (0.0004)}{2(208.0)} = 0.172 \text{ Np/m} = 1.49 \text{ dB/m.}$$

The conductivity of gold is $\sigma = 4.1 \times 10^7 \text{ S/m}$, so the surface resistance is

$$R_s = \sqrt{\frac{\omega\mu_0}{2\sigma}} = 0.0367 \Omega.$$

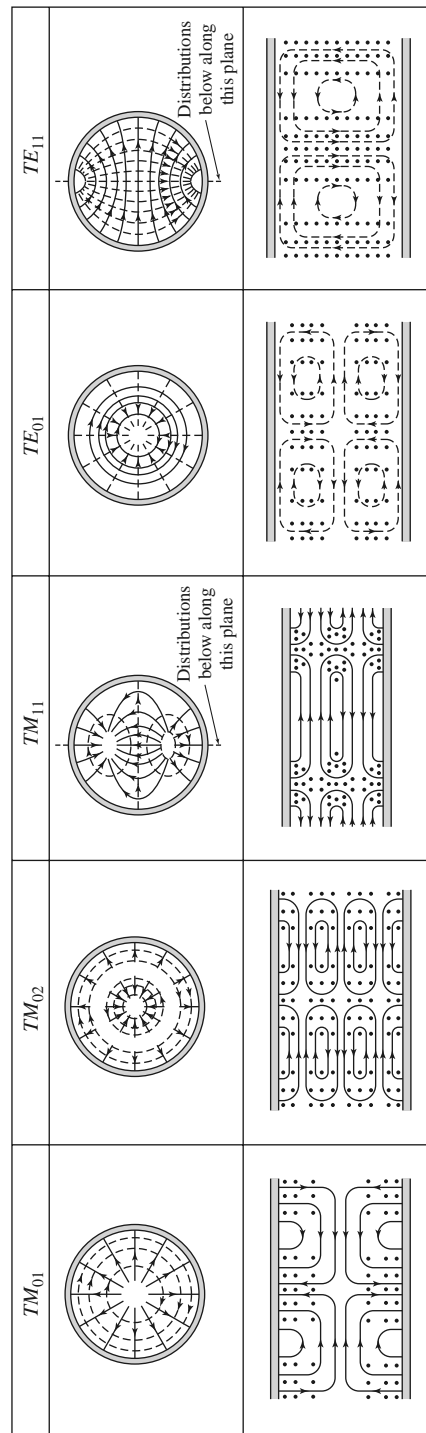


FIGURE 3.14 Field lines for some of the lower order modes of a circular waveguide.

Reprinted with permission from S. Ramo, J. R. Whinnery, and T. Van Duzer, *Fields and Waves in Communication Electronics*, Copyright © 1965 by John Wiley & Sons, Inc. Table 8.04.

Then from (3.133) the attenuation due to conductor loss is

$$\alpha_c = \frac{R_s}{ak\eta\beta} \left(k_c^2 + \frac{k^2}{p_{11}^2 - 1} \right) = 0.0672 \text{ Np/m} = 0.583 \text{ dB/m.}$$

The total attenuation is $\alpha = \alpha_d + \alpha_c = 2.07 \text{ dB/m}$, and the loss in the 30 cm length of guide is

$$\text{attenuation (dB)} = \alpha(\text{dB/m}) \times L(\text{m}) = (2.07)(0.3) = 0.62 \text{ dB.} \quad \blacksquare$$

3.5

COAXIAL LINE

TEM Modes

Although we have already discussed TEM mode propagation on a coaxial line in Chapter 2, we will briefly reconsider it here in the context of the general framework that is being used in this chapter.

The coaxial transmission line geometry is shown in Figure 3.15, where the inner conductor is at a potential of V_o volts and the outer conductor is at zero volts. From Section 3.1 we know that the fields can be derived from a scalar potential function, $\Phi(\rho, \phi)$, which is a solution to Laplace's equation (3.14). In cylindrical coordinates Laplace's equation takes the form

$$\frac{1}{\rho} \frac{\partial}{\partial \rho} \left(\rho \frac{\partial \Phi(\rho, \phi)}{\partial \rho} \right) + \frac{1}{\rho^2} \frac{\partial^2 \Phi(\rho, \phi)}{\partial \phi^2} = 0. \quad (3.143)$$

This equation must be solved for $\Phi(\rho, \phi)$ subject to the boundary conditions

$$\Phi(a, \phi) = V_o, \quad (3.144a)$$

$$\Phi(b, \phi) = 0. \quad (3.144b)$$

By the method of separation of variables, let $\Phi(\rho, \phi)$ be expressed in product form as

$$\Phi(\rho, \phi) = R(\rho)P(\phi). \quad (3.145)$$

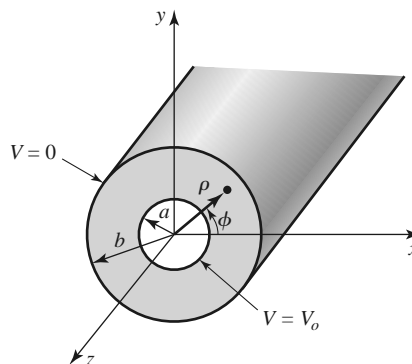


FIGURE 3.15 Coaxial line geometry.

Substituting (3.145) into (3.143) and dividing by RP gives

$$\frac{\rho}{R} \frac{\partial}{\partial \rho} \left(\rho \frac{dR}{d\rho} \right) + \frac{1}{P} \frac{d^2 P}{d\phi^2} = 0. \quad (3.146)$$

By the usual separation-of-variables argument, the two terms in (3.146) must be equal to constants, so that

$$\frac{\rho}{R} \frac{\partial}{\partial \rho} \left(\rho \frac{dR}{d\rho} \right) = -k_\rho^2, \quad (3.147)$$

$$\frac{1}{P} \frac{d^2 P}{d\phi^2} = -k_\phi^2, \quad (3.148)$$

$$k_\rho^2 + k_\phi^2 = 0. \quad (3.149)$$

The general solution to (3.148) is

$$P(\phi) = A \cos n\phi + B \sin n\phi, \quad (3.150)$$

where $k_\phi = n$ must be an integer since increasing ϕ by a multiple of 2π should not change the result. Now, because the boundary conditions of (3.144) do not vary with ϕ , the potential $\Phi(\rho, \phi)$ should not vary with ϕ . Thus, n must be zero. By (3.149), this implies that k_ρ must also be zero, so that the equation for $R(\rho)$ in (3.147) reduces to

$$\frac{\partial}{\partial \rho} \left(\rho \frac{dR}{d\rho} \right) = 0.$$

The solution for $R(\rho)$ is then

$$R(\rho) = C \ln \rho + D,$$

and so

$$\Phi(\rho, \phi) = C \ln \rho + D. \quad (3.151)$$

Applying the boundary conditions of (3.144) gives two equations for the constants C and D :

$$\Phi(a, \phi) = V_o = C \ln a + D, \quad (3.152a)$$

$$\Phi(b, \phi) = 0 = C \ln b + D. \quad (3.152b)$$

After solving for C and D , we can write the final solution for $\Phi(\rho, \phi)$ as

$$\Phi(\rho, \phi) = \frac{V_o \ln b/\rho}{\ln b/a}. \quad (3.153)$$

The \bar{E} and \bar{H} fields can now be found using (3.13) and (3.18), and the voltage, current, and characteristic impedance can be determined as in Chapter 2. Attenuation due to dielectric or conductor loss has already been treated in Chapter 2.

Higher Order Modes

The coaxial line, like the parallel plate waveguide, can also support TE and TM waveguide modes in addition to the TEM mode. In practice, these modes are usually cut off (evanescent), and so have only a reactive effect near discontinuities or sources, where they may be excited. It is important in practice, however, to be aware of the cutoff frequency of the lowest order waveguide-type modes to avoid the propagation of these modes. Undesirable

effects can occur if two or more modes with different propagation constants are propagating at the same time. Avoiding propagation of higher order modes sets an upper limit on the size of a coaxial cable or, equivalently, an upper limit on the frequency of operation for a given cable. This also affects the power handling capacity of a coaxial line (see the Point of Interest on power capacity of transmission lines).

We will derive the solution for the TE modes of the coaxial line; the TE₁₁ mode is the dominant waveguide mode of the coaxial line and so is of primary importance.

For TE modes, $E_z = 0$, and H_z satisfies the wave equation of (3.112):

$$\left(\frac{\partial^2}{\partial \rho^2} + \frac{1}{\rho} \frac{\partial}{\partial \rho} + \frac{1}{\rho^2} \frac{\partial^2}{\partial \phi^2} + k_c^2 \right) h_z(\rho, \phi) = 0, \quad (3.154)$$

where $H_z(\rho, \phi, z) = h_z(\rho, \phi)e^{-j\beta z}$, and $k_c^2 = k^2 - \beta^2$. The general solution to this equation, as derived in Section 3.4, is given by the product of (3.118) and (3.120):

$$h_z(\rho, \phi) = (A \sin n\phi + B \cos n\phi)(C J_n(k_c \rho) + D Y_n(k_c \rho)). \quad (3.155)$$

In this case, $a \leq \rho \leq b$, so we have no reason to discard the Y_n term. The boundary conditions are

$$E_\phi(\rho, \phi, z) = 0 \text{ for } \rho = a, b. \quad (3.156)$$

Using (3.110b) to find E_ϕ from H_z gives

$$E_\phi = \frac{j\omega\mu}{k_c} (A \sin n\phi + B \cos n\phi)[C J'_n(k_c \rho) + D Y'_n(k_c \rho)]e^{-j\beta z}. \quad (3.157)$$

Applying (3.156) to (3.157) gives two equations:

$$C J'_n(k_c a) + D Y'_n(k_c a) = 0, \quad (3.158a)$$

$$C J'_n(k_c b) + D Y'_n(k_c b) = 0. \quad (3.158b)$$

Because this is a homogeneous set of equations, the only nontrivial ($C \neq 0, D \neq 0$) solution occurs when the determinant is zero. Thus we must have

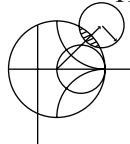
$$J'_n(k_c a) Y'_n(k_c b) = J'_n(k_c b) Y'_n(k_c a). \quad (3.159)$$

This is a characteristic (or eigenvalue) equation for k_c . The values of k_c that satisfy (3.159) then define the TE_{nm} modes of the coaxial line.

Equation (3.159) is a transcendental equation, which must be solved numerically for k_c . Figure 3.16 shows the result of such a solution for $n = 1$ for various b/a ratios. An approximate solution that is often used in practice is

$$k_c = \frac{2}{a + b}.$$

Once k_c is known, the propagation constant or cutoff frequency can be determined. Solutions for the TM modes can be found in a similar manner; the required determinantal equation is the same as (3.159), except for the derivatives. Field lines for the TEM and TE₁₁ modes of the coaxial line are shown in Figure 3.17.



EXAMPLE 3.3 HIGHER ORDER MODE OF A COAXIAL LINE

Consider a RG-401U semirigid coaxial cable, with inner and outer conductor diameters of 0.0645 in. and 0.215 in., and a Teflon dielectric with $\epsilon_r = 2.2$. What is the highest usable frequency before the TE₁₁ waveguide mode starts to propagate?

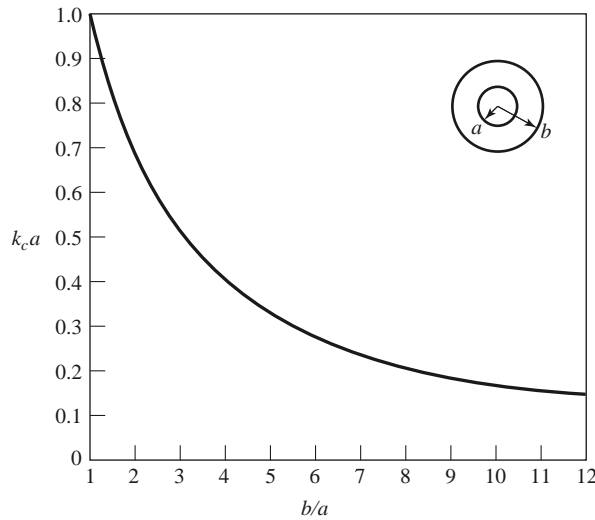


FIGURE 3.16 Normalized cutoff frequency of the dominant TE_{11} waveguide mode for a coaxial line.

Solution

We have

$$\frac{b}{a} = \frac{2b}{2a} = \frac{0.215}{0.0645} = 3.33.$$

From Figure 3.16 this value of b/a gives $k_c a = 0.45$ [the approximate result is $k_c a = 2/(1 + b/a) = 0.462$]. Thus, $k_c = 549.4 \text{ m}^{-1}$, and the cutoff frequency of the TE_{11} mode is

$$f_c = \frac{ck_c}{2\pi\sqrt{\epsilon_r}} = 17.7 \text{ GHz.}$$

In practice, a 5% safety margin is usually recommended, so

$$f_{\max} = (0.95)(17.7 \text{ GHz}) = 16.8 \text{ GHz.} \quad \blacksquare$$

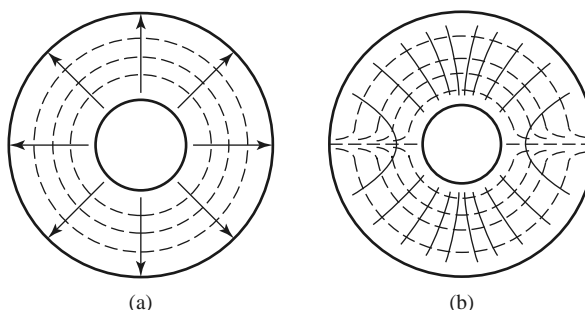
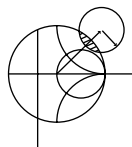


FIGURE 3.17 Field lines for the (a) TEM and (b) TE_{11} modes of a coaxial line.



POINT OF INTEREST: Coaxial Connectors

Most coaxial cables and connectors in common use have a $50\ \Omega$ characteristic impedance, with an exception being the $75\ \Omega$ cable used in television systems. The reasoning behind these choices is that an air-filled coaxial line has minimum attenuation for a characteristic impedance of about $77\ \Omega$ (Problem 2.27), while maximum power capacity occurs for a characteristic impedance of about $30\ \Omega$ (Problem 3.28). A $50\ \Omega$ characteristic impedance thus represents a compromise between minimum attenuation and maximum power capacity. Other requirements for coaxial connectors include low SWR, higher-order-mode-free operation at a high frequency, high repeatability after a connect–disconnect cycle, and mechanical strength. Connectors are used in pairs, with a male end and a female end (or plug and jack). The accompanying photo shows several types of commonly used coaxial connectors and adapters. From top left: Type-N, TNC, SMA, APC-7, and 2.4 mm.

Type-N: This connector was developed in 1942 and is named after its inventor, P. Neil, of Bell Labs. The outer diameter of the female end is about 0.625 in. The recommended upper frequency limit ranges from 11 to 18 GHz, depending on cable size. This rugged but large connector is often found on older equipment.

TNC: This is a threaded version of the very common BNC connector. Its use is limited to frequencies below 1 GHz.

SMA: The need for smaller and lighter connectors led to the development of this connector in the 1960s. The outer diameter of the female end is about 0.25 in. It can be used up to frequencies in the range of 18–25 GHz and is probably the most commonly used microwave connector today.

APC-7: This is a precision connector (Amphenol Precision Connector) that can repeatedly achieve SWR less than 1.04 at frequencies up to 18 GHz. The connectors are “sexless,” with butt contact between both inner conductors and outer conductors. This connector is most commonly used for measurement and instrumentation applications.

2.4 mm: The need for connectors at millimeter wave frequencies led to the development of several variations of the SMA connector. One of the most common is the 2.4 mm connector, which is useful to about 50 GHz. The size of this connector is similar to that of the SMA connector.

3.6

SURFACE WAVES ON A GROUNDED DIELECTRIC SHEET

We briefly discussed surface waves in Chapter 1 in connection with the field of a plane wave totally reflected from a dielectric interface, but surface waves can exist in a variety of geometries involving dielectric interfaces. Here we consider the TM and TE surface waves that can be excited along a grounded dielectric sheet. Other geometries that can be used as surface waveguides include an ungrounded dielectric sheet, a dielectric rod, a corrugated conductor, and a dielectric-coated conducting rod.

Surface waves are typified by a field that decays exponentially away from the dielectric surface, with most of the field contained in or near the dielectric. At higher frequencies the field generally becomes more tightly bound to the dielectric, making such waveguides practical. Because of the presence of the dielectric, the phase velocity of a surface wave is less than the velocity of light in a vacuum. Another reason for studying surface waves is that they may be excited on some types of planar transmission lines, such as microstrip line and slotline.

TM Modes

Figure 3.18 shows the geometry of a grounded dielectric slab waveguide. The dielectric sheet, of thickness d and relative permittivity ϵ_r , is assumed to be of infinite extent in the y and z directions. We will assume propagation in the $+z$ direction with an $e^{-j\beta z}$ propagation factor and no variation in the y direction ($\partial/\partial y = 0$).

Because there are two distinct regions, with and without a dielectric, we must separately consider the field in these regions and then match tangential fields across the interface. E_z must satisfy the wave equation of (3.25) in each region:

$$\left(\frac{\partial^2}{\partial x^2} + \epsilon_r k_0^2 - \beta^2 \right) e_z(x, y) = 0, \quad \text{for } 0 \leq x \leq d, \quad (3.160a)$$

$$\left(\frac{\partial^2}{\partial x^2} + k_0^2 - \beta^2 \right) e_z(x, y) = 0, \quad \text{for } d \leq x < \infty, \quad (3.160b)$$

where $E_z(x, y, z) = e_z(x, y) e^{-j\beta z}$.

We define the cutoff wave numbers for the two regions as

$$k_c^2 = \epsilon_r k_0^2 - \beta^2, \quad (3.161a)$$

$$h^2 = \beta^2 - k_0^2, \quad (3.161b)$$

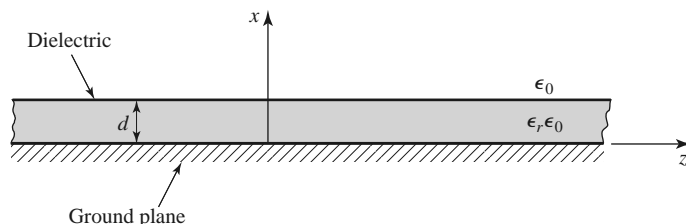


FIGURE 3.18 Geometry of a grounded dielectric sheet.

where the sign on h^2 has been selected in anticipation of an exponentially decaying result for $x > d$. Observe that the same propagation constant, β , has been used for both regions. This must be the case to achieve phase matching of the tangential fields at the $x = d$ interface for all values of z .

The general solutions to (3.160) are

$$e_z(x, y) = A \sin k_c x + B \cos k_c x, \quad \text{for } 0 \leq x \leq d \quad (3.162a)$$

$$e_z(x, y) = C e^{hx} + D e^{-hx}, \quad \text{for } d \leq x < \infty \quad (3.162b)$$

Note that these solutions are valid for k_c and h either real or imaginary; it will turn out that both k_c and h are real because of the choice of definitions in (3.161).

The boundary conditions that must be satisfied are

$$E_z(x, y, z) = 0, \quad \text{at } x = 0, \quad (3.163a)$$

$$E_z(x, y, z) < \infty, \quad \text{as } x \rightarrow \infty, \quad (3.163b)$$

$$E_z(x, y, z) \text{ continuous at } x = d, \quad (3.163c)$$

$$H_y(x, y, z) \text{ continuous at } x = d. \quad (3.163d)$$

From (3.23), $H_x = E_y = H_z = 0$. Condition (3.163a) implies that $B = 0$ in (3.162a). Condition (3.163b) is a result of a requirement for finite fields (and energy) infinitely far away from a source and implies that $C = 0$. The continuity of E_z leads to

$$A \sin k_c d = D e^{-hd}, \quad (3.164a)$$

while (3.23b) must be used to apply continuity to H_y , to obtain

$$\frac{\epsilon_r A}{k_c} \cos k_c d = \frac{D}{h} e^{-hd}. \quad (3.164b)$$

For a nontrivial solution, the determinant of the two equations of (3.164) must vanish, leading to

$$k_c \tan k_c d = \epsilon_r h. \quad (3.165)$$

Eliminating β from (3.161a) and (3.161b) gives

$$k_c^2 + h^2 = (\epsilon_r - 1) k_0^2. \quad (3.166)$$

Equations (3.165) and (3.166) constitute a set of simultaneous transcendental equations that must be solved for the propagation constants k_c and h , given k_0 and ϵ_r . These equations are easily solved numerically, but Figure 3.19 shows a graphical representation of the solutions. Multiplying both sides of (3.166) by d^2 gives

$$(k_c d)^2 + (h d)^2 = (\epsilon_r - 1) (k_0 d)^2,$$

which is the equation of a circle in the $k_c d, h d$ plane, as shown in Figure 3.19. The radius of the circle is $\sqrt{\epsilon_r - 1} k_0 d$, which is proportional to the electrical thickness of the dielectric sheet. Multiplying (3.165) by d gives

$$k_c d \tan k_c d = \epsilon_r h d,$$

which is also plotted in Figure 3.19. The intersection of these curves implies a solution to both (3.165) and (3.166). Observe that k_c may be positive or negative; from (3.162a) this is seen to merely change the sign of the constant A . As $\sqrt{\epsilon_r - 1} k_0 d$ becomes larger, the circle may intersect more than one branch of the tangent function, implying that more than

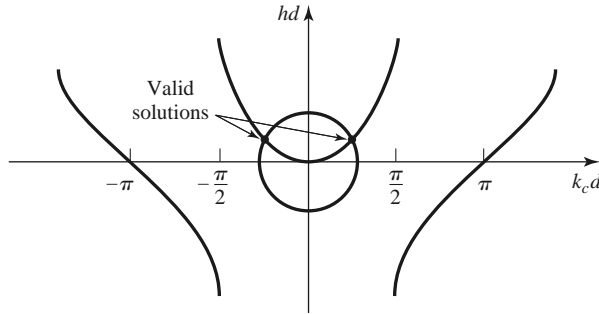


FIGURE 3.19 Graphical solution of the transcendental equation for the cutoff frequency of a TM surface wave mode of the grounded dielectric sheet.

one TM mode can propagate. Solutions for negative h , however, must be excluded since we assumed h was positive real when applying boundary condition (3.163b).

For any nonzero-thickness sheet with a relative permittivity greater than unity, there is at least one propagating TM mode, which we will call the TM_0 mode. This is the dominant mode of the dielectric slab waveguide, and it has a zero cutoff frequency. (Although for $k_0 = 0$, $k_c = h = 0$, and all fields vanish.) From Figure 3.19 it can be seen that the next TM mode, the TM_1 mode, will not begin to propagate until the radius of the circle becomes greater than π . The cutoff frequency of the TM_n mode can then be derived as

$$f_c = \frac{nc}{2d\sqrt{\epsilon_r - 1}}, \quad n = 0, 1, 2, \dots \quad (3.167)$$

Once k_c and h have been found for a particular surface wave mode, the field expressions can be found as

$$E_z(x, y, z) = \begin{cases} A \sin k_c x e^{-j\beta z} & \text{for } 0 \leq x \leq d \\ A \sin k_c d e^{-h(x-d)} e^{-j\beta z} & \text{for } d \leq x < \infty, \end{cases} \quad (3.168a)$$

$$E_x(x, y, z) = \begin{cases} \frac{-j\beta}{k_c} A \cos k_c x e^{-j\beta z} & \text{for } 0 \leq x \leq d \\ \frac{-j\beta}{h} A \sin k_c d e^{-h(x-d)} e^{-j\beta z} & \text{for } d \leq x < \infty, \end{cases} \quad (3.168b)$$

$$H_y(x, y, z) = \begin{cases} \frac{-j\omega\epsilon_0\epsilon_r}{k_c} A \cos k_c x e^{-j\beta z} & \text{for } 0 \leq x \leq d \\ \frac{-j\omega\epsilon_0}{h} A \sin k_c d e^{-h(x-d)} e^{-j\beta z} & \text{for } d \leq x < \infty. \end{cases} \quad (3.168c)$$

TE Modes

TE modes can also be supported by the grounded dielectric sheet. The H_z field satisfies the wave equations

$$\left(\frac{\partial^2}{\partial x^2} + k_c^2 \right) h_z(x, y) = 0, \quad \text{for } 0 \leq x \leq d, \quad (3.169a)$$

$$\left(\frac{\partial^2}{\partial x^2} - h^2 \right) h_z(x, y) = 0, \quad \text{for } d \leq x < \infty, \quad (3.169b)$$

with $H_z(x, y, z) = h_z(x, y)e^{-j\beta z}$ and k_c^2 and h^2 defined in (3.161a) and (3.161b). As for the TM modes, the general solutions to (3.169) are

$$h_z(x, y) = A \sin k_c x + B \cos k_c x, \quad (3.170a)$$

$$h_z(x, y) = Ce^{hx} + De^{-hx}. \quad (3.170b)$$

To satisfy the radiation condition, $C = 0$. Using (3.19d) to find E_y from H_z leads to $A = 0$ for $E_y = 0$ at $x = 0$ and to the equation

$$\frac{-B}{k_c} \sin k_c d = \frac{D}{h} e^{-hd} \quad (3.171a)$$

for continuity of E_y at $x = d$. Continuity of H_z at $x = d$ gives

$$B \cos k_c d = D e^{-hd}. \quad (3.171b)$$

Simultaneously solving (3.171a) and (3.171b) leads to the determinantal equation

$$-k_c \cot k_c d = h. \quad (3.172)$$

From (3.161a) and (3.161b) we also have that

$$k_c^2 + h^2 = (\epsilon_r - 1)k_0^2. \quad (3.173)$$

Equations (3.172) and (3.173) must be solved simultaneously for the variables k_c and h . Equation (3.173) again represents circles in the $k_c d$, hd plane, while (3.172) can be rewritten as

$$-k_c d \cot k_c d = hd,$$

and plotted as a family of curves in the $k_c d$, hd plane, as shown in Figure 3.20. Because negative values of h must be excluded, we see from Figure 3.20 that the first TE mode does not start to propagate until the radius of the circle, $\sqrt{\epsilon_r - 1}k_0 d$, becomes greater than $\pi/2$. The cutoff frequency of the TE_n modes can then be found as

$$f_c = \frac{(2n-1)c}{4d\sqrt{\epsilon_r - 1}} \quad \text{for } n = 1, 2, 3, \dots \quad (3.174)$$

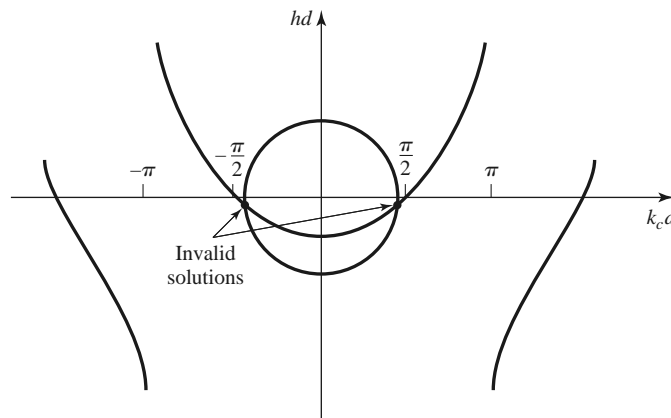


FIGURE 3.20 Graphical solution of the transcendental equation for the cutoff frequency of a TE surface wave mode. The figure depicts a mode below cutoff.

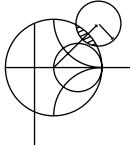
Comparing with (3.167) shows that the order of propagation for the TM_n and TE_n modes is $\text{TM}_0, \text{TE}_1, \text{TM}_1, \text{TE}_2, \text{TM}_2, \dots$.

After finding the constants k_c and h , the field expressions can be derived as

$$H_z(x, y, z) = \begin{cases} B \cos k_c x e^{-j\beta z} & \text{for } 0 \leq x \leq d \\ B \cos k_c d e^{-h(x-d)} e^{-j\beta z} & \text{for } d \leq x < \infty, \end{cases} \quad (3.175a)$$

$$H_x(x, y, z) = \begin{cases} \frac{j\beta}{k_c} B \sin k_c x e^{-j\beta z} & \text{for } 0 \leq x \leq d \\ \frac{-j\beta}{h} B \cos k_c d e^{-h(x-d)} e^{-j\beta z} & \text{for } d \leq x < \infty, \end{cases} \quad (3.175b)$$

$$E_y(x, y, z) = \begin{cases} \frac{-j\omega\mu_0}{k_c} B \sin k_c x e^{-j\beta z} & \text{for } 0 \leq x \leq d \\ \frac{j\omega\mu_0}{h} B \cos k_c d e^{-h(x-d)} e^{-j\beta z} & \text{for } d \leq x < \infty. \end{cases} \quad (3.175c)$$



EXAMPLE 3.4 SURFACE WAVE PROPAGATION CONSTANTS

Calculate and plot the propagation constants of the first three propagating surface wave modes of a grounded dielectric sheet with $\epsilon_r = 2.55$, for $d/\lambda_0 = 0$ to 1.2.

Solution

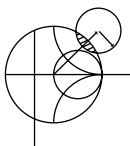
The first three propagating surface wave modes are the TM_0 , TE_1 , and TM_1 modes. The cutoff frequencies for these modes can be found from (3.167) and (3.174) as

$$\text{TM}_0: f_c = 0 \implies \frac{d}{\lambda_0} = 0,$$

$$\text{TE}_1: f_c = \frac{c}{4d\sqrt{\epsilon_r - 1}} \implies \frac{d}{\lambda_0} = \frac{1}{(4\sqrt{\epsilon_r - 1})},$$

$$\text{TM}_1: f_c = \frac{c}{2d\sqrt{\epsilon_r - 1}} \implies \frac{d}{\lambda_0} = \frac{1}{(2\sqrt{\epsilon_r - 1})}.$$

The propagation constants can be found from the numerical solution of (3.165) and (3.166) for the TM modes and (3.172) and (3.173) for the TE modes. This can be done with a relatively simple root-finding algorithm (see the Point of Interest on root-finding algorithms); the results are shown in Figure 3.21. ■



POINT OF INTEREST: Root-Finding Algorithms

In several examples throughout this book we will need to numerically find the root of a transcendental equation, so it may be useful to review two relatively simple but effective algorithms for doing this. Both methods can be easily programmed.

In the *interval-halving method* the root of $f(x) = 0$ is first bracketed between the values x_1 and x_2 . These values can often be estimated from the problem under consideration. If a single root lies between x_1 and x_2 , then $f(x_1)f(x_2) < 0$. An estimate, x_3 , of the root is made by halving the interval between x_1 and x_2 . Thus,

$$x_3 = \frac{x_1 + x_2}{2}.$$

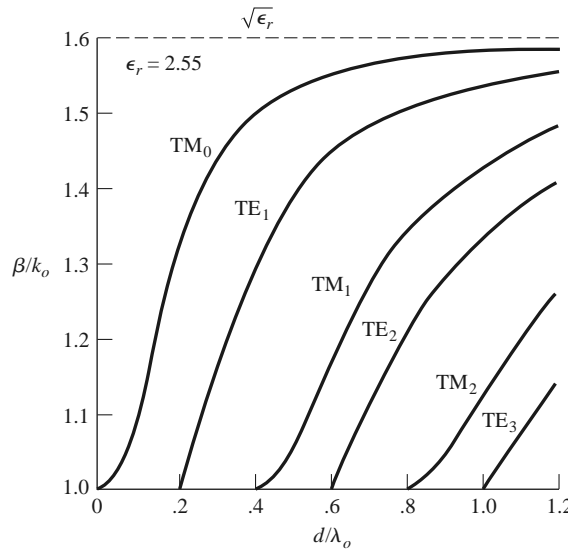


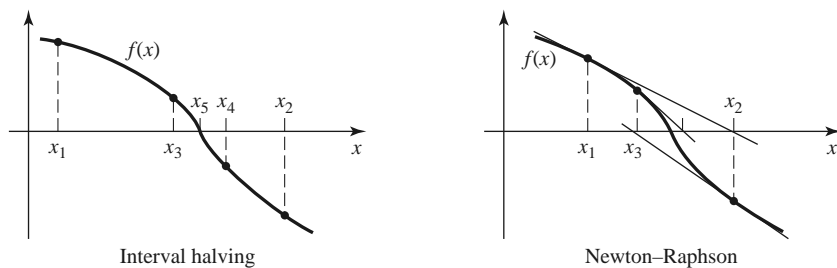
FIGURE 3.21 Surface wave propagation constants for a grounded dielectric slab with $\epsilon_r = 2.55$.

If $f(x_1)f(x_3) < 0$, then the root must lie in the interval $x_1 < x < x_3$; if $f(x_3)f(x_2) < 0$, the root must be in the interval $x_3 < x < x_2$. A new estimate, x_4 , can be made by halving the appropriate interval, and this process is repeated until the location of the root has been determined with the desired accuracy. The accompanying figure illustrates this algorithm for several iterations.

The *Newton–Raphson* method begins with an estimate, x_1 , of the root of $f(x) = 0$. Then a new estimate, x_2 , is obtained from the formula

$$x_2 = x_1 - \frac{f(x_1)}{f'(x_1)},$$

where $f'(x_1)$ is the derivative of $f(x)$ at x_1 . This result is easily derived from a two-term Taylor series expansion of $f(x)$ near $x = x_1$: $f(x) = f(x_1) + (x - x_1)f'(x_1)$. It can also be interpreted geometrically as fitting a straight line at $x = x_1$ with the same slope as $f(x)$ at this point; this line then intercepts the x -axis at $x = x_2$, as shown in the figure. Reapplying the above formula gives improved estimates of the root. Convergence is generally much faster than with the interval-halving method, but a disadvantage is that the derivative of $f(x)$ is required; this can often be computed numerically. The *Newton–Raphson* technique can easily be applied to the case where the root is complex (a situation that occurs, for example, when finding the propagation constant of a line or guide with loss).



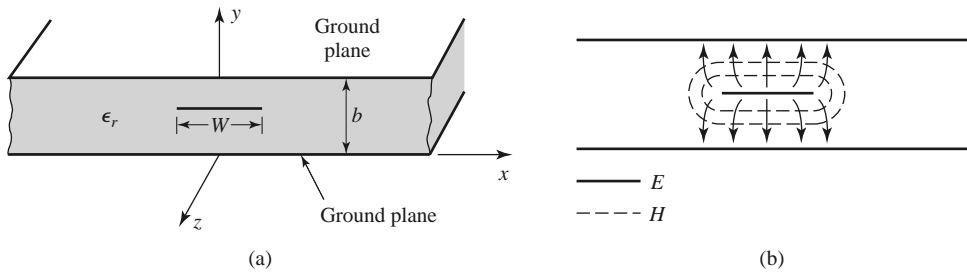


FIGURE 3.22 Stripline transmission line. (a) Geometry. (b) Electric and magnetic field lines.

3.7 STRIPLINE

Stripline is a planar type of transmission line that lends itself well to microwave integrated circuitry, miniaturization, and photolithographic fabrication. The geometry of stripline is shown in Figure 3.22a. A thin conducting strip of width W is centered between two wide conducting ground planes of separation b , and the region between the ground planes is filled with a dielectric material. In practice stripline is usually constructed by etching the center conductor on a grounded dielectric substrate of thickness $b/2$ and then covering with another grounded substrate. Variations of the basic geometry of Figure 3.22a include stripline with differing dielectric substrate thicknesses (*asymmetric stripline*) or different dielectric constants (*inhomogeneous stripline*). Air dielectric is sometimes used when it is necessary to minimize loss. An example of a stripline circuit is shown in Figure 3.23.

Because stripline has two conductors and a homogeneous dielectric, it supports a TEM wave, and this is the usual mode of operation. Like parallel plate guide and coaxial line, however, stripline can also support higher order waveguide modes. These can usually be avoided in practice by restricting both the ground plane spacing and the sidewall width to less than $\lambda_d/2$. Shorting vias between the ground planes are often used to enforce this condition relative to the sidewall width. Shorting vias should also be used to eliminate higher order modes that can be generated when an asymmetry is introduced between the ground planes (e.g., when a surface-mounted coaxial transition is used).

Intuitively, one can think of stripline as a sort of “flattened-out” coax—both have a center conductor completely enclosed by an outer conductor and are uniformly filled with a dielectric medium. A sketch of the field lines for stripline is shown in Figure 3.22b.

The geometry of stripline does not lend itself to the simple analyses that were used for previously treated transmission lines and waveguides. Because we will be concerned primarily with the TEM mode of stripline, an electrostatic analysis is sufficient to give the propagation constant and characteristic impedance. An exact solution of Laplace’s equation is possible by a conformal mapping approach [6], but the procedure and results are cumbersome. Instead, we will present closed-form expressions that give good approximations to the exact results and then discuss an approximate numerical technique for solving Laplace’s equation for a geometry similar to stripline.

Formulas for Propagation Constant, Characteristic Impedance, and Attenuation

From Section 3.1 we know that the phase velocity of a TEM mode is given by

$$v_p = 1/\sqrt{\mu_0 \epsilon_0 \epsilon_r} = c/\sqrt{\epsilon_r}, \quad (3.176)$$

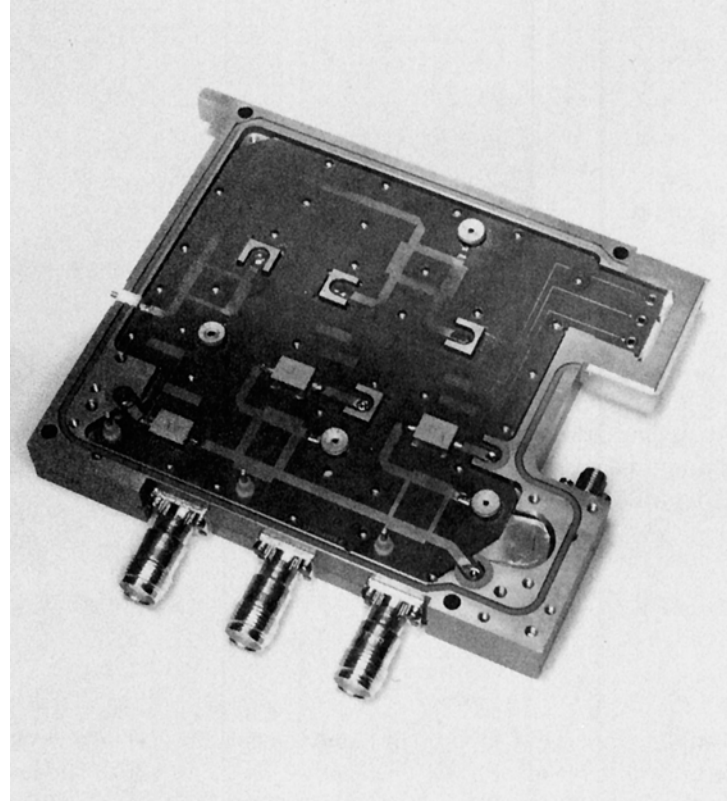


FIGURE 3.23 Photograph of a stripline circuit assembly (cover removed), showing four quadrature hybrids, open-circuit tuning stubs, and coaxial transitions.

and thus the propagation constant of stripline is

$$\beta = \frac{\omega}{v_p} = \omega \sqrt{\mu_0 \epsilon_0 \epsilon_r} = \sqrt{\epsilon_r} k_0. \quad (3.177)$$

In (3.176), $c = 3 \times 10^8$ m/sec is the speed of light in free-space. Using (2.13) and (2.16) allows us to write the characteristic impedance of a transmission line as

$$Z_0 = \sqrt{\frac{L}{C}} = \frac{\sqrt{LC}}{C} = \frac{1}{v_p C}, \quad (3.178)$$

where L and C are the inductance and capacitance per unit length of the line. Thus, we can find Z_0 if we know C . As mentioned previously, Laplace's equation can be solved by conformal mapping to find the capacitance per unit length of stripline, but the resulting solution involves complicated special functions [6], so for practical computations simple formulas have been developed by curve fitting to the exact solution [6, 7]. The resulting formula for characteristic impedance is

$$Z_0 = \frac{30\pi}{\sqrt{\epsilon_r}} \frac{b}{W_e + 0.441b}, \quad (3.179a)$$

where W_e is the *effective width* of the center conductor given by

$$\frac{W_e}{b} = \frac{W}{b} - \begin{cases} 0 & \text{for } \frac{W}{b} > 0.35 \\ (0.35 - W/b)^2 & \text{for } \frac{W}{b} < 0.35. \end{cases} \quad (3.179b)$$

These formulas assume a strip with zero thickness and are quoted as being accurate to about 1% of the exact results. It is seen from (3.179) that the characteristic impedance decreases as the strip width W increases.

When designing stripline circuits one usually needs to find the strip width, given the characteristic impedance (and height b and relative permittivity ϵ_r), which requires the inverse of the formulas in (3.179). Such formulas have been derived as

$$\frac{W}{b} = \begin{cases} x & \text{for } \sqrt{\epsilon_r}Z_0 < 120 \Omega \\ 0.85 - \sqrt{0.6 - x} & \text{for } \sqrt{\epsilon_r}Z_0 > 120 \Omega, \end{cases} \quad (3.180a)$$

where

$$x = \frac{30\pi}{\sqrt{\epsilon_r}Z_0} - 0.441. \quad (3.180b)$$

Since stripline is a TEM line, the attenuation due to dielectric loss is of the same form as that for other TEM lines and is given in (3.30). The attenuation due to conductor loss can be found by the perturbation method or Wheeler's incremental inductance rule. An approximate result is

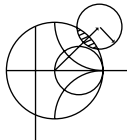
$$\alpha_c = \begin{cases} \frac{2.7 \times 10^{-3} R_s \epsilon_r Z_0}{30\pi(b-t)} A & \text{for } \sqrt{\epsilon_r}Z_0 < 120 \Omega \\ \frac{0.16 R_s}{Z_0 b} B & \text{for } \sqrt{\epsilon_r}Z_0 > 120 \Omega \end{cases} \text{ Np/m,} \quad (3.181)$$

with

$$A = 1 + \frac{2W}{b-t} + \frac{1}{\pi} \frac{b+t}{b-t} \ln \left(\frac{2b-t}{t} \right),$$

$$B = 1 + \frac{b}{(0.5W + 0.7t)} \left(0.5 + \frac{0.414t}{W} + \frac{1}{2\pi} \ln \frac{4\pi W}{t} \right),$$

where t is the thickness of the strip.



EXAMPLE 3.5 STRIPLINE DESIGN

Find the width for a 50Ω copper stripline conductor with $b = 0.32$ cm and $\epsilon_r = 2.20$. If the dielectric loss tangent is 0.001 and the operating frequency is 10 GHz, calculate the attenuation in dB/λ . Assume a conductor thickness of $t = 0.01$ mm.

Solution

Because $\sqrt{\epsilon_r}Z_0 = \sqrt{2.2}(50) = 74.2 < 120$ and $x = 30\pi/(\sqrt{\epsilon_r}Z_0) - 0.441 = 0.830$, (3.180) gives the strip width as $W = bx = (0.32)(0.830) = 0.266$ cm.

At 10 GHz, the wave number is

$$k = \frac{2\pi f \sqrt{\epsilon_r}}{c} = 310.6 \text{ m}^{-1}.$$

From (3.30) the dielectric attenuation is

$$\alpha_d = \frac{k \tan \delta}{2} = \frac{(310.6)(0.001)}{2} = 0.155 \text{ Np/m.}$$

The surface resistance of copper at 10 GHz is $R_s = 0.026 \Omega$. Then from (3.181) the conductor attenuation is

$$\alpha_c = \frac{2.7 \times 10^{-3} R_s \epsilon_r Z_0 A}{30\pi(b-t)} = 0.122 \text{ Np/m,}$$

since $A = 4.74$. The total attenuation constant is

$$\alpha = \alpha_d + \alpha_c = 0.277 \text{ Np/m.}$$

In dB,

$$\alpha(\text{dB}) = 20 \log e^\alpha = 2.41 \text{ dB/m.}$$

At 10 GHz, the wavelength on the stripline is

$$\lambda = \frac{c}{\sqrt{\epsilon_r} f} = 2.02 \text{ cm,}$$

so in terms of wavelength the attenuation is

$$\alpha(\text{dB}) = (2.41)(0.0202) = 0.049 \text{ dB}/\lambda. \quad \blacksquare$$

An Approximate Electrostatic Solution

Many practical problems in microwave engineering are very complicated and do not lend themselves to straightforward analytic solutions but require some sort of numerical approach. Thus it is useful for the student to become aware of such techniques; we will introduce such methods when appropriate throughout this book, beginning with a numerical solution for the characteristic impedance of stripline.

We know that the fields of the TEM mode on stripline must satisfy Laplace's equation, (3.11), in the region between the two parallel plates. The idealized stripline geometry of Figure 3.22a extends to $\pm\infty$, which makes the analysis more difficult. Because we suspect, from the field line drawing of Figure 3.22b, that the field lines do not extend very far away from the center conductor, we can simplify the geometry by truncating the plates beyond some distance, say $|x| > a/2$, and placing metal walls on the sides. Thus, the geometry we will analyze is shown in Figure 3.24, where $a \gg b$, so that the fields around the center

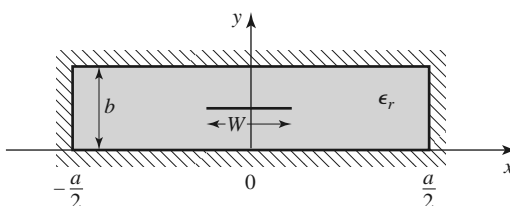


FIGURE 3.24 Geometry of enclosed stripline.

conductor are not perturbed by the sidewalls. We then have a closed finite region in which the potential $\Phi(x, y)$ satisfies Laplace's equation,

$$\nabla_t^2 \Phi(x, y) = 0 \quad \text{for } |x| \leq a/2, 0 \leq y \leq b, \quad (3.182)$$

with the boundary conditions

$$\Phi(x, y) = 0, \quad \text{at } x = \pm a/2, \quad (3.183a)$$

$$\Phi(x, y) = 0, \quad \text{at } y = 0, b. \quad (3.183b)$$

Laplace's equation can be solved by the method of separation of variables. Because the center conductor at $y = b/2$ will contain a surface charge density, the potential $\Phi(x, y)$ will have a slope discontinuity there because $\bar{D} = -\epsilon_0 \epsilon_r \nabla_t \Phi$ is discontinuous at $y = b/2$. Therefore, separate solutions for $\Phi(x, y)$ must be found for $0 < y < b/2$ and $b/2 < y < b$. The general solutions for $\Phi(x, y)$ in these two regions can be written as

$$\Phi(x, y) = \begin{cases} \sum_{\substack{n=1 \\ \text{odd}}}^{\infty} A_n \cos \frac{n\pi x}{a} \sinh \frac{n\pi y}{a} & \text{for } 0 \leq y \leq b/2 \\ \sum_{\substack{n=1 \\ \text{odd}}}^{\infty} B_n \cos \frac{n\pi x}{a} \sinh \frac{n\pi}{a} (b - y) & \text{for } b/2 \leq y \leq b. \end{cases} \quad (3.184)$$

Only the odd- n terms are needed in (3.184) because the solution is an even function of x . The reader can verify by substitution that (3.184) satisfies Laplace's equation in the two regions and satisfies the boundary conditions of (3.183).

The potential must be continuous at $y = b/2$, which from (3.184) leads to

$$A_n = B_n. \quad (3.185)$$

The remaining set of unknown coefficients, A_n , can be found by solving for the charge density on the center strip. Because $E_y = -\partial \Phi / \partial y$, we have

$$E_y = \begin{cases} -\sum_{\substack{n=1 \\ \text{odd}}}^{\infty} A_n \left(\frac{n\pi}{a} \right) \cos \frac{n\pi x}{a} \cosh \frac{n\pi y}{a} & \text{for } 0 \leq y \leq b/2 \\ \sum_{\substack{n=1 \\ \text{odd}}}^{\infty} A_n \left(\frac{n\pi}{a} \right) \cos \frac{n\pi x}{a} \cosh \frac{n\pi}{a} (b - y) & \text{for } b/2 \leq y \leq b. \end{cases} \quad (3.186)$$

The surface charge density on the strip at $y = b/2$ is

$$\begin{aligned} \rho_s &= D_y(x, y = b/2^+) - D_y(x, y = b/2^-) \\ &= \epsilon_0 \epsilon_r [E_y(x, y = b/2^+) - E_y(x, y = b/2^-)] \\ &= 2\epsilon_0 \epsilon_r \sum_{\substack{n=1 \\ \text{odd}}}^{\infty} A_n \left(\frac{n\pi}{a} \right) \cos \frac{n\pi x}{a} \cosh \frac{n\pi b}{2a}, \end{aligned} \quad (3.187)$$

which is seen to be a Fourier series in x for the surface charge density, ρ_s , on the strip at $y = b/2$. If we know the surface charge density we could easily find the unknown constants, A_n , and then the capacitance. We do not know the exact surface charge density, but we can make a good guess by approximating it as a constant over the width of the strip,

$$\rho_s(x) = \begin{cases} 1 & \text{for } |x| < W/2 \\ 0 & \text{for } |x| > W/2. \end{cases} \quad (3.188)$$

Equating this to (3.187) and using the orthogonality properties of the $\cos(n\pi x/a)$ functions gives the constants A_n as

$$A_n = \frac{2a \sin(n\pi W/2a)}{(n\pi)^2 \epsilon_0 \epsilon_r \cosh(n\pi b/2a)}. \quad (3.189)$$

The voltage of the strip conductor relative to the bottom conductor can be found by integrating the vertical electric field from $y = 0$ to $b/2$. Because the solution is approximate, this voltage is not constant over the width of the strip but varies with position, x . Rather than choosing the voltage at an arbitrary position, we can obtain an improved result by averaging the voltage over the width of the strip:

$$V_{\text{avg}} = \frac{1}{W} \int_{-W/2}^{W/2} \int_0^{b/2} E_y(x, y) dy dx = \sum_{\substack{n=1 \\ \text{odd}}}^{\infty} A_n \left(\frac{2a}{n\pi W} \right) \sin \frac{n\pi W}{2a} \sinh \frac{n\pi b}{2a}. \quad (3.190)$$

The total charge per unit length on the center conductor is

$$Q = \int_{-W/2}^{W/2} \rho_s(x) dx = W \text{ Coul/m}, \quad (3.191)$$

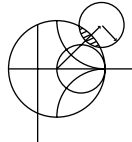
so the capacitance per unit length of the stripline is

$$C = \frac{Q}{V_{\text{avg}}} = \frac{W}{\sum_{\substack{n=1 \\ \text{odd}}}^{\infty} A_n \left(\frac{2a}{n\pi W} \right) \sin \frac{n\pi W}{2a} \sinh \frac{n\pi b}{2a}} \text{ F/m}. \quad (3.192)$$

Finally, the characteristic impedance is given by

$$Z_0 = \sqrt{\frac{L}{C}} = \frac{\sqrt{LC}}{C} = \frac{1}{v_p C} = \frac{\sqrt{\epsilon_r}}{c C},$$

where $c = 3 \times 10^8$ m/sec.



EXAMPLE 3.6 NUMERICAL CALCULATION OF STRIPLINE IMPEDANCE

Evaluate the above expressions for a stripline having $\epsilon_r = 2.55$ and $a = 100b$ to find the characteristic impedance for $W/b = 0.25$ to 5.0. Compare with the results from (3.179).

Solution

A computer program was written to evaluate (3.192). The series was truncated after 500 terms, and the results for Z_0 are as follows.

W/b	Z_0, Ω		
	Numerical, Eq. (3.192)	Formula, Eq. (3.179)	Commercial CAD
0.25	90.9	86.6	85.3
0.50	66.4	62.7	61.7
1.0	43.6	41.0	40.2
2.0	25.5	24.2	24.4
5.0	11.1	10.8	11.9

We see that the results are in reasonable agreement with the closed-form equations of (3.179) and the results from a commercial CAD package, particularly for wider strips where the charge density is closer to uniform. Better results could be obtained if more sophisticated estimates were used for the charge density. ■

3.8

MICROSTRIP LINE

Microstrip line is one of the most popular types of planar transmission lines primarily because it can be fabricated by photolithographic processes and is easily miniaturized and integrated with both passive and active microwave devices. The geometry of a microstrip line is shown in Figure 3.25a. A conductor of width W is printed on a thin, grounded dielectric substrate of thickness d and relative permittivity ϵ_r ; a sketch of the field lines is shown in Figure 3.25b.

If the dielectric substrate were not present ($\epsilon_r = 1$), we would have a two-wire line consisting of a flat strip conductor over a ground plane, embedded in a homogeneous medium (air). This would constitute a simple TEM transmission line with phase velocity $v_p = c$ and propagation constant $\beta = k_0$.

The presence of the dielectric, particularly the fact that the dielectric does not fill the region above the strip ($y > d$), complicates the behavior and analysis of microstrip line. Unlike stripline, where all the fields are contained within a homogeneous dielectric region, microstrip has some (usually most) of its field lines in the dielectric region between the strip conductor and the ground plane and some fraction in the air region above the substrate. For this reason microstrip line cannot support a pure TEM wave since the phase velocity of TEM fields in the dielectric region would be $c/\sqrt{\epsilon_r}$, while the phase velocity of TEM fields in the air region would be c , so a phase-matching condition at the dielectric–air interface would be impossible to enforce.

In actuality, the exact fields of a microstrip line constitute a hybrid TM-TE wave and require more advanced analysis techniques than we are prepared to deal with here. In most practical applications, however, the dielectric substrate is electrically very thin ($d \ll \lambda$), and so the fields are quasi-TEM. In other words, the fields are essentially the same as those of the static (DC) case. Thus, good approximations for the phase velocity, propagation constant, and characteristic impedance can be obtained from static, or *quasi-static*, solutions. Then the phase velocity and propagation constant can be expressed as

$$v_p = \frac{c}{\sqrt{\epsilon_r}}, \quad (3.193)$$

$$\beta = k_0 \sqrt{\epsilon_r}, \quad (3.194)$$

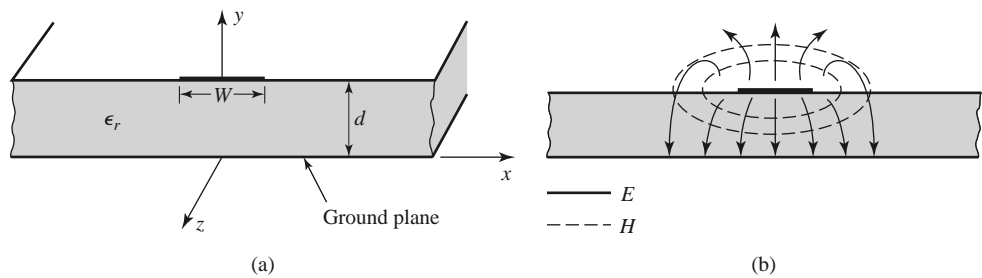


FIGURE 3.25 Microstrip transmission line. (a) Geometry. (b) Electric and magnetic field lines.

where ϵ_e is the *effective dielectric constant* of the microstrip line. Because some of the field lines are in the dielectric region and some are in air, the effective dielectric constant satisfies the relation

$$1 < \epsilon_e < \epsilon_r$$

and depends on the substrate dielectric constant, the substrate thickness, the conductor width, and the frequency.

We will present approximate design formulas for the effective dielectric constant, characteristic impedance, and attenuation of microstrip line; these results are curve-fit approximations to rigorous quasi-static solutions [8, 9]. Then we will discuss additional aspects of microstrip lines, including frequency-dependent effects, higher order modes, and parasitic effects.

Formulas for Effective Dielectric Constant, Characteristic Impedance, and Attenuation

The effective dielectric constant of a microstrip line is given approximately by

$$\epsilon_e = \frac{\epsilon_r + 1}{2} + \frac{\epsilon_r - 1}{2} \frac{1}{\sqrt{1 + 12d/W}}. \quad (3.195)$$

The effective dielectric constant can be interpreted as the dielectric constant of a homogeneous medium that equivalently replaces the air and dielectric regions of the microstrip line, as shown in Figure 3.26. The phase velocity and propagation constant are then given by (3.193) and (3.194).

Given the dimensions of the microstrip line, the characteristic impedance can be calculated as

$$Z_0 = \begin{cases} \frac{60}{\sqrt{\epsilon_e}} \ln \left(\frac{8d}{W} + \frac{W}{4d} \right) & \text{for } W/d \leq 1 \\ \frac{120\pi}{\sqrt{\epsilon_e} [W/d + 1.393 + 0.667 \ln (W/d + 1.444)]} & \text{for } W/d \geq 1. \end{cases} \quad (3.196)$$

For a given characteristic impedance Z_0 and dielectric constant ϵ_r , the W/d ratio can be found as

$$\frac{W}{d} = \begin{cases} \frac{8e^A}{e^{2A} - 2} & \text{for } W/d < 2 \\ \frac{2}{\pi} \left[B - 1 - \ln(2B - 1) + \frac{\epsilon_r - 1}{2\epsilon_r} \left\{ \ln(B - 1) + 0.39 - \frac{0.61}{\epsilon_r} \right\} \right] & \text{for } W/d > 2, \end{cases} \quad (3.197)$$

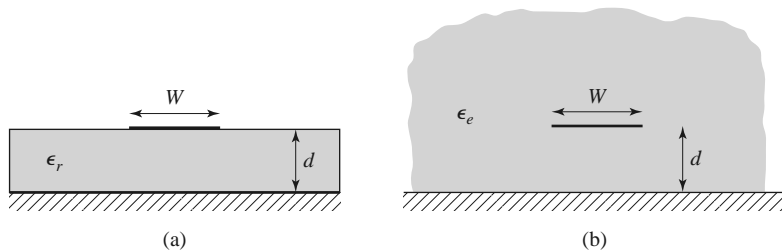


FIGURE 3.26 Equivalent geometry of a quasi-TEM microstrip line. (a) Original geometry. (b) Equivalent geometry, where the dielectric substrate of relative permittivity ϵ_r is replaced with a homogeneous medium of effective relative permittivity ϵ_e .

where

$$A = \frac{Z_0}{60} \sqrt{\frac{\epsilon_r + 1}{2}} + \frac{\epsilon_r - 1}{\epsilon_r + 1} \left(0.23 + \frac{0.11}{\epsilon_r} \right)$$

$$B = \frac{377\pi}{2Z_0\sqrt{\epsilon_r}}.$$

Considering a microstrip line as a quasi-TEM line, we can determine the attenuation due to dielectric loss as

$$\alpha_d = \frac{k_0 \epsilon_r (\epsilon_e - 1) \tan \delta}{2\sqrt{\epsilon_e} (\epsilon_r - 1)} \text{ Np/m}, \quad (3.198)$$

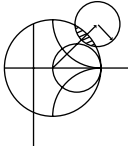
where $\tan \delta$ is the loss tangent of the dielectric. This result is derived from (3.30) by multiplying by a “filling factor,”

$$\frac{\epsilon_r (\epsilon_e - 1)}{\epsilon_e (\epsilon_r - 1)},$$

which accounts for the fact that the fields around the microstrip line are partly in air (lossless) and partly in the dielectric (lossy). The attenuation due to conductor loss is given approximately by [8]

$$\alpha_c = \frac{R_s}{Z_0 W} \text{ Np/m}, \quad (3.199)$$

where $R_s = \sqrt{\omega \mu_0 / 2\sigma}$ is the surface resistivity of the conductor. For most microstrip substrates, conductor loss is more significant than dielectric loss; exceptions may occur, however, with some semiconductor substrates.



EXAMPLE 3.7 MICROSTRIP LINE DESIGN

Design a microstrip line on a 0.5 mm alumina substrate ($\epsilon_r = 9.9$, $\tan \delta = 0.001$) for a 50Ω characteristic impedance. Find the length of this line required to produce a phase delay of 270° at 10 GHz, and compute the total loss on this line, assuming copper conductors. Compare the results obtained from the approximate formulas of (3.195)–(3.199) with those from a microwave CAD package.

Solution

First find W/d for $Z_0 = 50 \Omega$, and initially guess that $W/d < 2$. From (3.197),

$$A = 2.142, \quad W/d = 0.9654.$$

So the condition that $W/d < 2$ is satisfied; otherwise we would use the expression for $W/d > 2$. Then the required line width is $W = 0.9654d = 0.483$ mm. From (3.195) the effective dielectric constant is $\epsilon_e = 6.665$. The line length, ℓ , for a 270° phase shift is found as

$$\phi = 270^\circ = \beta \ell = \sqrt{\epsilon_e} k_0 \ell,$$

$$k_0 = \frac{2\pi f}{c} = 209.4 \text{ m}^{-1},$$

$$\ell = \frac{270^\circ (\pi / 180^\circ)}{\sqrt{\epsilon_e} k_0} = 8.72 \text{ mm}.$$

Attenuation due to dielectric loss is found from (3.198) as $\alpha_d = 0.255 \text{ Np/m} = 0.022 \text{ dB/cm}$. The surface resistivity for copper at 10 GHz is 0.026Ω , and the attenuation due to conductor loss is, from (3.199), $\alpha_c = 0.0108 \text{ Np/cm} = 0.094 \text{ dB/cm}$. The total loss on the line is then 0.101 dB.

A commercial microwave CAD package gives the following results: $W = 0.478 \text{ mm}$, $\epsilon_e = 6.83$, $\ell = 8.61 \text{ mm}$, $\alpha_d = 0.022 \text{ dB/cm}$, and $\alpha_c = 0.054 \text{ dB/cm}$. The approximate formulas give results that are within a few percent of the CAD data for linewidth, effective dielectric constant, line length, and dielectric attenuation. The greatest discrepancy occurs for the attenuation constant for conductor loss. ■

Frequency-Dependent Effects and Higher Order Modes

The results for the parameters of microstrip line presented in the previous section were based on the quasi-static approximation and are strictly valid only at DC (or very low frequencies). At higher frequencies a number of effects can occur that lead to variations from the quasi-static results for effective dielectric constant, characteristic impedance, and attenuation of microstrip line. In addition, new effects can arise, such as higher order modes and parasitic reactances.

Because microstrip line is not a true TEM line, its propagation constant is not a linear function of frequency, meaning that the effective dielectric constant varies with frequency. The electromagnetic field that exists on microstrip line involves a hybrid coupling of TM and TE modes, complicated by the boundary condition imposed by the air and dielectric substrate interface. In addition, the current on the strip conductor is not uniform across the width of the strip, and this distribution varies with frequency. The thickness of the strip conductor also has an effect on the current distribution and hence affects the line parameters (especially the conductor loss).

The variation with frequency of the parameters of a transmission line is important for several reasons. First, if the variation is significant it becomes important to know and use the parameters at the particular frequency of interest to avoid errors in design or analysis. Typically, for microstrip line, the frequency variation of the effective dielectric constant is more significant than the variation of characteristic impedance, both in terms of relative change and the relative effect on performance. A change in the effective dielectric constant may have a substantial effect on the phase delay through a long section of line, while a small change in characteristic impedance has the primary effect of introducing a small impedance mismatch. Second, a variation in line parameters with frequency means that different frequency components of a broadband signal will propagate differently. A variation in phase velocity, for example, means that different frequency components will arrive at the output of the line at different times, leading to *signal dispersion* and distortion of the input signal. Third, because of the complexity of modeling these effects, approximate formulas are generally useful only for a limited range of frequency and line parameters, and numerical computer models are usually more accurate and useful.

There are a number of approximate formulas, developed from numerical computer solutions and/or experimental data, that have been suggested for predicting the frequency variation of microstrip line parameters [8, 9]. A popular frequency-dependent model for the effective dielectric constant has a form similar to the following formula [8]:

$$\epsilon_e(f) = \epsilon_r - \frac{\epsilon_r - \epsilon_e(0)}{1 + G(f)}, \quad (3.200)$$

where $\epsilon_e(f)$ represents the frequency-dependent effective dielectric constant, ϵ_r is the relative permittivity of the substrate, and $\epsilon_e(0)$ is the effective dielectric constant of the line at

DC, as given by (3.195). The function $G(f)$ can take various forms, but one suggested in reference [8] is that $G(f) = g(f/f_p)^2$, with $g = 0.6 + 0.009 Z_0$ and $f_p = Z_0/8\pi d$ (Z_0 is in ohms, f is in GHz, and d is in cm). It can be seen from the form of (3.200) that $\epsilon_e(f)$ reduces to the DC value $\epsilon_e(0)$ when $f = 0$ and increases toward ϵ_r as frequency increases.

Approximate formulas like the above were primarily developed in the years before computer-aided design tools for RF and microwave engineering became commonly available (see the Point of Interest on computer-aided design in Chapter 4). Such tools usually give accurate results for a wide range of line parameters and today are usually preferred over closed-form approximations.

Another potential difficulty with microstrip line is that it may support several types of higher order modes, particularly at higher frequencies. Some of these are directly related to the TM and TE surface waves modes that were discussed in Section 3.6, while others are related to waveguide-type modes in the cross section of the line.

The TM_0 surface wave mode for a grounded dielectric substrate has a zero cutoff frequency, as we know from (3.167). Because some of the field lines of this mode are aligned with the field lines of the quasi-TEM mode of a microstrip line, it is possible for coupling to occur from the desired microstrip mode to a surface wave, leading to excess power loss and possibly undesired coupling to adjacent microstrip elements. Because the fields of the TM_0 surface wave are zero at DC, there is little coupling to the quasi-TEM microstrip mode until a critical frequency is reached. Studies have shown that this threshold frequency is greater than zero and less than the cutoff frequency of the TM_1 surface wave mode. A commonly used approximation is [8]

$$f_{T1} \simeq \frac{c}{2\pi d} \sqrt{\frac{2}{\epsilon_r - 1}} \tan^{-1} \epsilon_r. \quad (3.201)$$

For ϵ_r ranging from 1 to 10, (3.201) gives a frequency that is 35% to 66% of f_{c1} , the cutoff frequency of the TM_1 surface wave mode.

When a microstrip circuit has transverse discontinuities (such as bends, junctions, or even step changes in width), the transverse currents on the conductors that are generated may allow coupling to TE surface wave modes. Most practical microstrip circuits involve such discontinuities, so this type of coupling is often important. The minimum threshold frequency where such coupling becomes important is given by the cutoff of the TE_1 surface wave, from (3.174):

$$f_{T2} \simeq \frac{c}{4d\sqrt{\epsilon_r - 1}}. \quad (3.202)$$

For wide microstrip lines, it is possible to excite a transverse resonance along the x axis of the microstrip line below the strip in the dielectric region because the sides below the strip conductor appear approximately as magnetic walls. This condition occurs when the width is about $\lambda/2$ in the dielectric, but because of field fringing the effective width of the strip is somewhat larger than the physical width. A rough approximation for the effective width is $W + d/2$, so the approximate threshold frequency for transverse resonance is

$$f_{T3} \simeq \frac{c}{\sqrt{\epsilon_r} (2W + d)}. \quad (3.203)$$

It is rare that a microstrip line is wide enough to approach this limit in practice.

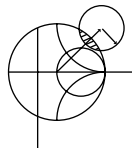
Finally, a parallel plate-type waveguide mode may propagate when the vertical spacing between the strip conductor and ground plane approaches $\lambda/2$ in the dielectric. Thus, an

approximation for the threshold frequency for this mode (valid for wide microstrip lines) can be given as

$$f_{T4} \simeq \frac{c}{2d\sqrt{\epsilon_r}}. \quad (3.204)$$

Thinner microstrip lines will have more fringing field that effectively lengthens the path between the strip and ground plane, thus reducing the threshold frequency by as much as 50%.

The net effect of the threshold frequencies given in (3.201)–(3.204) is to impose an upper frequency limit of operation for a given microstrip geometry. This limit is a function of the substrate thickness, dielectric constant, and strip width.



EXAMPLE 3.8 FREQUENCY DEPENDENCE OF EFFECTIVE DIELECTRIC CONSTANT

Use the approximate formula of (3.200) to plot the change in effective dielectric constant over frequency for a 25Ω microstrip line on a substrate having a relative permittivity of 10.0 and a thickness of 0.65 mm. Compare the approximate data with results from a CAD model for frequencies up to 20 GHz. Compare the calculated phase delay at 10 GHz through a 1.093 cm length of line when using $\epsilon_e(0)$ versus $\epsilon_e(10 \text{ GHz})$.

Solution

The required linewidth for a 25Ω impedance is $w = 2.00 \text{ mm}$. The effective dielectric constant for this line at low frequencies can be found from (3.195) to be $\epsilon_e(0) = 7.53$. A short computer program was used to calculate the effective dielectric constant as a function of frequency using (3.200), and the result is shown in Figure 3.27. Comparison with a commercial microwave CAD package shows that the approximate model is reasonably accurate up to about 10 GHz but gives an overestimate at higher frequencies.

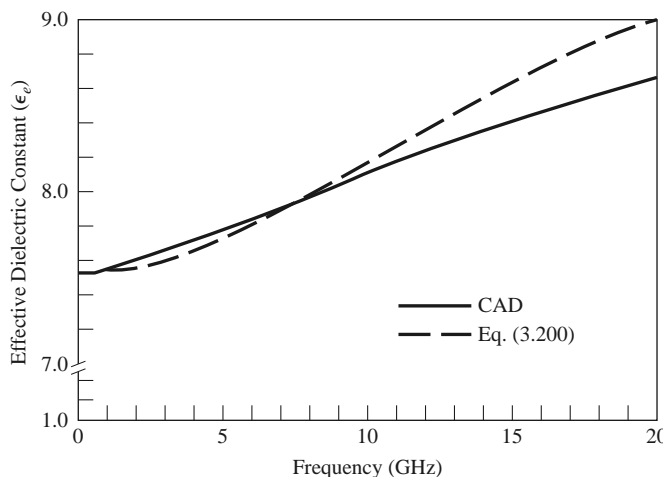


FIGURE 3.27 Effective dielectric constant versus frequency for the microstrip line of Example 3.8, comparing the approximate model of (3.200) with data from a computer-aided design package.

Using an effective dielectric constant of $\epsilon_e(0) = 7.53$, we find the phase delay through a 1.093 cm length of line to be $\phi_0 = \sqrt{\epsilon_e(0)}k_0\ell = 360^\circ$. The effective dielectric constant at 10 GHz is 8.120 (CAD), with a corresponding phase delay of $\phi_{10} = \sqrt{\epsilon_e(10 \text{ GHz})}k_0\ell = 374^\circ$ —an error of about 14° . ■

3.9

THE TRANSVERSE RESONANCE TECHNIQUE

According to the general solutions of Maxwell's equations for TE or TM waves given in Section 3.1, a uniform waveguide structure always has a propagation constant of the form

$$\beta = \sqrt{k^2 - k_c^2} = \sqrt{k^2 - k_x^2 - k_y^2}, \quad (3.205)$$

where $k_c = \sqrt{k_x^2 + k_y^2}$ is the cutoff wave number of the guide and, for a given mode, is a fixed function of the cross-sectional geometry of the guide. Thus, if we know k_c we can determine the propagation constant of the guide. In previous sections we determined k_c by solving the wave equation in the guide, subject to the appropriate boundary conditions. Although this technique is very powerful and general, it can be complicated for complex waveguides, especially if dielectric layers are present. In addition, the wave equation solution gives a complete field description inside the waveguide, which is often more information than we really need if we are only interested in the propagation constant of the guide. The *transverse resonance technique* employs a transmission line model of the transverse cross section of the waveguide and gives a much simpler and more direct solution for the cutoff frequency. This is another example where circuit and transmission line theory offers a simplified alternative to a field theory solution.

The transverse resonance procedure is based on the fact that in a waveguide at cutoff, the fields form standing waves in the transverse plane of the guide, as can be inferred from the “bouncing plane wave” interpretation of waveguide modes discussed in Section 3.2. This situation can be modeled with an equivalent transmission line circuit operating at resonance. One of the conditions of such a resonant line is the fact that, at any point on the line, the sum of the input impedances seen looking to either side must be zero. That is,

$$Z_{\text{in}}^r(x) + Z_{\text{in}}^\ell(x) = 0 \quad \text{for all } x, \quad (3.206)$$

where $Z_{\text{in}}^r(x)$ and $Z_{\text{in}}^\ell(x)$ are the input impedances seen looking to the right and left, respectively, at any point x on the resonant line.

The transverse resonance technique only gives results for the cutoff frequency of the guide. If fields or attenuation due to conductor loss are needed, the complete field theory solution will be required. The procedure will now be illustrated with an example.

TE_{0n} Modes of a Partially Loaded Rectangular Waveguide

The transverse resonance technique is particularly useful when the guide contains dielectric layers because the boundary conditions at the dielectric interfaces, which require the solution of simultaneous algebraic equations in the field theory approach, can be easily handled as junctions of different transmission lines. As an example, consider a rectangular waveguide partially filled with dielectric, as shown in Figure 3.28. To find the cutoff frequencies for the TE_{0n} modes, the equivalent transverse resonance circuit shown in the figure can be used. The line for $0 < y < t$ represents the dielectric-filled part of the guide

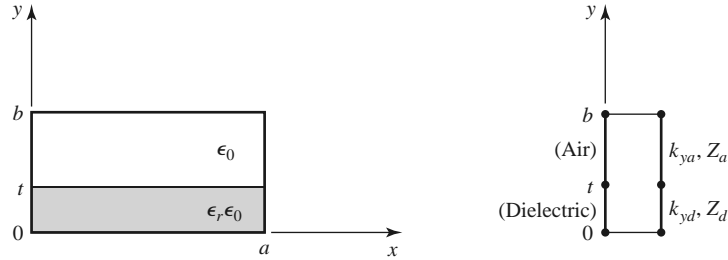


FIGURE 3.28 A rectangular waveguide partially filled with dielectric and the transverse resonance equivalent circuit.

and has a transverse propagation constant k_{yd} and a characteristic impedance for TE modes given by

$$Z_d = \frac{k\eta}{k_{yd}} = \frac{k_0\eta_0}{k_{yd}}, \quad (3.207a)$$

where $k_0 = \omega\sqrt{\mu_0\epsilon_0}$ and $\eta_0 = \sqrt{\mu_0/\epsilon_0}$. For $t < y < b$, the guide is air filled and has a transverse propagation constant k_{ya} and an equivalent characteristic impedance given by

$$Z_a = \frac{k_0\eta_0}{k_{ya}}. \quad (3.207b)$$

Applying condition (3.206) yields

$$k_{ya} \tan k_{yd}t + k_{yd} \tan k_{ya}(b-t) = 0. \quad (3.208)$$

This equation contains two unknowns, k_{ya} and k_{yd} . An additional equation is obtained from the fact that the longitudinal propagation constant, β , must be the same in both regions for phase matching of the tangential fields at the dielectric interface. Thus, with $k_x = 0$,

$$\beta = \sqrt{\epsilon_r k_0^2 - k_{yd}^2} = \sqrt{k_0^2 - k_{ya}^2},$$

or

$$\epsilon_r k_0^2 - k_{yd}^2 = k_0^2 - k_{ya}^2. \quad (3.209)$$

Equations (3.208) and (3.209) can be solved (numerically or graphically) to obtain k_{yd} and k_{ya} . There will be an infinite number of solutions, corresponding to the n dependence (number of variations in y) of the TE_{0n} mode.

3.10 WAVE VELOCITIES AND DISPERSION

We have so far encountered two types of velocities related to the propagation of electromagnetic waves:

- The speed of light in a medium ($1/\sqrt{\mu\epsilon}$)
- The phase velocity ($v_p = \omega/\beta$)

The speed of light in a medium is the velocity at which a plane wave would propagate in that medium, while the phase velocity is the speed at which a constant phase point travels. For a TEM plane wave, these two velocities are identical, but for other types of guided wave propagation the phase velocity may be greater or less than the speed of light.

If the phase velocity and attenuation of a line or guide are constants that do not change with frequency, then the phase of a signal that contains more than one frequency component will not be distorted. If the phase velocity is different for different frequencies, then the individual frequency components will not maintain their original phase relationships as they propagate down the transmission line or waveguide, and signal distortion will occur. Such an effect is called *dispersion* since different phase velocities allow the “faster” waves to lead in phase relative to the “slower” waves, and the original phase relationships will gradually be dispersed as the signal propagates down the line. In such a case, there is no single phase velocity that can be attributed to the signal as a whole. However, if the bandwidth of the signal is relatively small or if the dispersion is not too severe, a *group velocity* can be defined in a meaningful way. This velocity can be used to describe the speed at which the signal propagates.

Group Velocity

As discussed earlier, the physical interpretation of group velocity is the velocity at which a narrowband signal propagates. We will derive the relation of group velocity to the propagation constant by considering a signal $f(t)$ in the time domain. The Fourier transform of this signal is defined as

$$F(\omega) = \int_{-\infty}^{\infty} f(t)e^{-j\omega t} dt, \quad (3.210a)$$

and the inverse transform is

$$f(t) = \frac{1}{2\pi} \int_{-\infty}^{\infty} F(\omega)e^{j\omega t} d\omega. \quad (3.210b)$$

Now consider the transmission line or waveguide on which the signal $f(t)$ is propagating as a linear system, with a transfer function $Z(\omega)$ that relates the output, $F_o(\omega)$, of the line to the input, $F(\omega)$, of the line, as shown in Figure 3.29. Thus,

$$F_o(\omega) = Z(\omega)F(\omega). \quad (3.211)$$

For a lossless matched transmission line or waveguide, the transfer function $Z(\omega)$ can be expressed as

$$Z(\omega) = Ae^{-j\beta z} = |Z(\omega)|e^{-j\psi}, \quad (3.212)$$

where A is a constant and β is the propagation constant of the line or guide.

The time domain representation of the output signal, $f_o(t)$, can then be written as

$$f_o(t) = \frac{1}{2\pi} \int_{-\infty}^{\infty} F(\omega)|Z(\omega)|e^{j(\omega t - \psi)} d\omega. \quad (3.213)$$

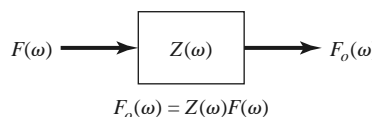


FIGURE 3.29 A transmission line or waveguide represented as a linear system with transfer function $Z(\omega)$.

If $|Z(\omega)| = A$ is a constant and the phase ψ of $Z(\omega)$ is a linear function of ω , say $\psi = a\omega$, the output can be expressed as

$$f_o(t) = \frac{1}{2\pi} \int_{-\infty}^{\infty} AF(\omega) e^{j\omega(t-a)} d\omega = Af(t-a), \quad (3.214)$$

which is seen to be a replica of $f(t)$, except for an amplitude factor A and time shift a . Thus, a transfer function of the form $Z(\omega) = Ae^{-j\omega a}$ does not distort the input signal. A lossless TEM wave has a propagation constant $\beta = \omega/c$, which is of this form, so a TEM line is *dispersionless* and does not lead to signal distortion. If the TEM line is lossy, however, the attenuation may be a function of frequency, which could lead to signal distortion.

Now consider a narrowband input signal of the form

$$s(t) = f(t) \cos \omega_0 t = \operatorname{Re} \left\{ f(t) e^{j\omega_0 t} \right\}, \quad (3.215)$$

which represents an amplitude-modulated carrier wave of frequency ω_0 . Assume that the highest frequency component of $f(t)$ is ω_m , where $\omega_m \ll \omega_0$. The Fourier transform, $S(\omega)$, of $s(t)$, is

$$S(\omega) = \int_{-\infty}^{\infty} f(t) e^{-j\omega_0 t} e^{j\omega t} dt = F(\omega - \omega_0), \quad (3.216)$$

where we have used the complex form of the input signal as expressed in (3.215). We will need to take the real part of the output inverse transform to obtain the time domain output signal. The spectra of $F(\omega)$ and $S(\omega)$ are depicted in Figure 3.30.

The output signal spectrum is

$$S_o(\omega) = AF(\omega - \omega_0) e^{-j\beta z}, \quad (3.217)$$

and in the time domain,

$$\begin{aligned} s_o(t) &= \frac{1}{2\pi} \operatorname{Re} \int_{-\infty}^{\infty} S_o(\omega) e^{j\omega t} d\omega \\ &= \frac{1}{2\pi} \operatorname{Re} \int_{\omega_0 - \omega_m}^{\omega_0 + \omega_m} AF(\omega - \omega_0) e^{j(\omega t - \beta z)} d\omega. \end{aligned} \quad (3.218)$$

In general, the propagation constant β may be a complicated function of ω . However, if $F(\omega)$ is narrowband ($\omega_m \ll \omega_0$), then β can often be linearized by using a Taylor series expansion about ω_0 :

$$\beta(\omega) = \beta(\omega_0) + \left. \frac{d\beta}{d\omega} \right|_{\omega=\omega_0} (\omega - \omega_0) + \frac{1}{2} \left. \frac{d^2\beta}{d\omega^2} \right|_{\omega=\omega_0} (\omega - \omega_0)^2 + \dots \quad (3.219)$$

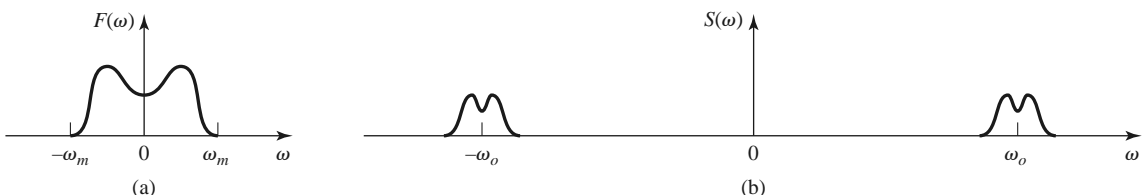


FIGURE 3.30 Fourier spectra of the signals (a) $f(t)$ and (b) $s(t)$.

Retaining the first two terms gives

$$\beta(\omega) \simeq \beta_o + \beta'_o(\omega - \omega_o), \quad (3.220)$$

where

$$\beta_o = \beta(\omega_o),$$

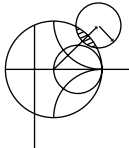
$$\beta'_o = \left. \frac{d\beta}{d\omega} \right|_{\omega=\omega_o}.$$

After a change of variables to $y = \omega - \omega_o$, the expression for $s_o(t)$ becomes

$$\begin{aligned} s_o(t) &= \frac{A}{2\pi} \operatorname{Re} \left\{ e^{j(\omega_o t - \beta_o z)} \int_{-\omega_m}^{\omega_m} F(y) e^{j(t - \beta'_o z)y} dy \right\} \\ &= A \operatorname{Re} \left\{ f(t - \beta'_o z) e^{j(\omega_o t - \beta_o z)} \right\} \\ &= A f(t - \beta'_o z) \cos(\omega_o t - \beta_o z), \end{aligned} \quad (3.221)$$

which is a time-shifted replica of the original modulation envelope, $f(t)$, of (3.215). The velocity of this envelope is the group velocity, v_g :

$$v_g = \frac{1}{\beta'_o} = \left. \left(\frac{d\beta}{d\omega} \right)^{-1} \right|_{\omega=\omega_o}. \quad (3.222)$$



EXAMPLE 3.9 WAVEGUIDE WAVE VELOCITIES

Calculate the group velocity for a waveguide mode propagating in an air-filled guide. Compare this velocity to the phase velocity and speed of light.

Solution

The propagation constant for a mode in an air-filled waveguide is

$$\beta = \sqrt{k_0^2 - k_c^2} = \sqrt{(\omega/c)^2 - k_c^2}.$$

Taking the derivative with respect to frequency gives

$$\frac{d\beta}{d\omega} = \frac{\omega/c^2}{\sqrt{(\omega/c)^2 - k_c^2}} = \frac{k_o}{c\beta},$$

so from (3.234) the group velocity is

$$v_g = \left(\frac{d\beta}{d\omega} \right)^{-1} = \frac{c\beta}{k_0}.$$

The phase velocity is $v_p = \omega/\beta = ck_0/\beta$. Since $\beta < k_0$, we have that $v_g < c < v_p$, which indicates that the phase velocity of a waveguide mode may be greater than the speed of light, but the group velocity (the velocity of a narrow-band signal) will be less than the speed of light. ■

3.11

SUMMARY OF TRANSMISSION LINES AND WAVEGUIDES

We have discussed a variety of transmission lines and waveguides in this chapter, and here we will summarize some of the basic properties of these transmission media and their relative advantages in a broader context.

TABLE 3.6 Comparison of Common Transmission Lines and Waveguides

Characteristic	Coax	Waveguide	Stripline	Microstrip
Modes: Preferred	TEM	TE ₁₀	TEM	Quasi-TEM
Other	TM,TE	TM,TE	TM,TE	Hybrid TM,TE
Dispersion	None	Medium	None	Low
Bandwidth	High	Low	High	High
Loss	Medium	Low	High	High
Power capacity	Medium	High	Low	Low
Physical size	Large	Large	Medium	Small
Ease of fabrication	Medium	Medium	Easy	Easy
Integration with	Hard	Hard	Fair	Easy

We made a distinction between TEM, TM, and TE waves and saw that transmission lines and waveguides can be categorized according to which type of waves they can support. We saw that TEM waves are nondispersive, with no cutoff frequency, while TM and TE waves exhibit dispersion and generally have nonzero cutoff frequencies. Other electrical considerations include bandwidth, attenuation, and power-handling capacity. Mechanical factors are also very important, however, and include such considerations as physical size (volume and weight), ease of fabrication (cost), and the ability to be integrated with other devices (active or passive). Table 3.6 compares several types of transmission media with regard to these considerations; this table only gives general guidelines, as specific cases may give better or worse results than those indicated.

Other Types of Lines and Guides

Although we have discussed the most common types of waveguides and transmission lines, there are many other guides and lines (and many variations) that we are not able to present in detail. A few of the more popular types are briefly mentioned here.

Ridge waveguide: The practical bandwidth of rectangular waveguide is slightly less than an octave (a 2:1 frequency range). This is because the TE₂₀ mode begins to propagate at a frequency equal to twice the cutoff frequency of the TE₁₀ mode. The ridge waveguide, shown in Figure 3.31, consists of a rectangular waveguide loaded with conducting ridges on the top and/or bottom walls. This loading tends to lower the cutoff frequency of the dominant mode, leading to increased bandwidth and better (more constant) impedance characteristics. Ridge waveguides are often used for impedance matching purposes, where

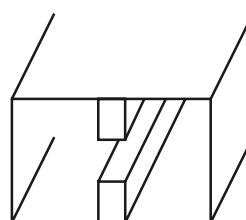


FIGURE 3.31 Cross section of a ridge waveguide.

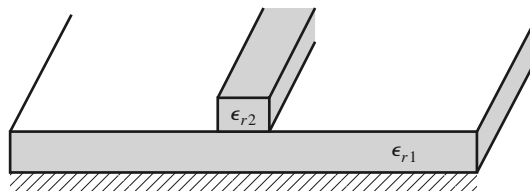


FIGURE 3.32 Dielectric waveguide geometry.

the ridge may be tapered along the length of the guide. The presence of the ridge, however, reduces the power-handling capacity of the waveguide.

Dielectric waveguide: As we have seen from our study of surface waves, metallic conductors are not necessary to confine and support a propagating electromagnetic field. The dielectric waveguide shown in Figure 3.32 is another example of such a guide, where ϵ_{r2} , the dielectric constant of the ridge, is usually greater than ϵ_{r1} , the dielectric constant of the substrate. The fields are thus mostly confined to the ridge and the surrounding area. This type of guide supports TM and TE modes, and is convenient for miniaturization and integration with active devices. Its small size makes it useful for millimeter wave to optical frequencies, although it can be very lossy at bends or junctions in the ridge line. Many variations in this basic geometry are possible.

Slotline: Slotline is another one of the many possible types of planar transmission lines. The geometry of a slotline is shown in Figure 3.33. It consists of a thin slot in the ground plane on one side of a dielectric substrate. Thus, like microstrip line, the two conductors of slotline lead to a quasi-TEM type of mode. The width of the slot controls the characteristic impedance of the line.

Coplanar waveguide: The coplanar waveguide, shown in Figure 3.34, is similar to the slotline, and can be viewed as a slotline with a third conductor centered in the slot region. Because of the presence of this additional conductor, this type of line can support even or odd quasi-TEM modes, depending on whether the electric fields in the two slots are in the opposite direction or the same direction. Coplanar waveguides are particularly useful for fabricating active circuitry due to the presence of the center conductor and the close proximity of the ground planes.

Covered microstrip: Many variations of the basic microstrip line geometry are possible, but one of the more common is the covered microstrip, shown in Figure 3.35. The metallic cover plate is often used for electrical shielding and physical protection of the microstrip circuitry and is usually situated several substrate thicknesses away from the circuit. Its presence, however, can perturb the operation of the circuit enough so that its effect must be taken into account during design.

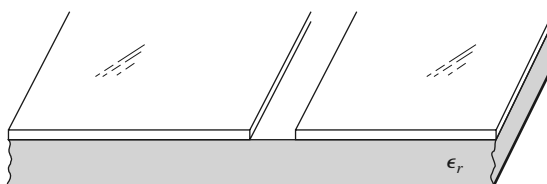


FIGURE 3.33 Geometry of a printed slotline.

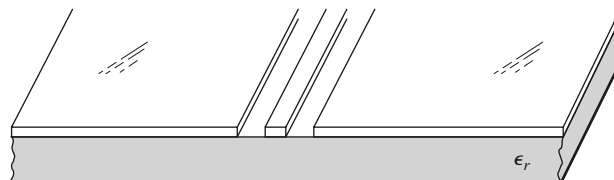
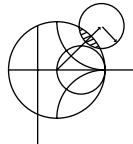


FIGURE 3.34 Coplanar waveguide geometry.

**POINT OF INTEREST:** Power Capacity of Transmission Lines

The power-handling capacity of an air-filled transmission line or waveguide is usually limited by voltage breakdown, which occurs at a field strength of about $E_d = 3 \times 10^6$ V/m for room temperature air at sea level pressure. Thermal effects may also serve to limit the power capacity of some types of lines.

In an air-filled coaxial line the electric field varies as $E_\rho = V_o/(\rho \ln b/a)$, which has a maximum at $\rho = a$ (at the inner conductor). Thus the maximum voltage before breakdown is

$$V_{\max} = E_d a \ln \frac{b}{a} \quad (\text{peak-to-peak}),$$

and the maximum power capacity is then

$$P_{\max} = \frac{V_{\max}^2}{2Z_0} = \frac{\pi a^2 E_d^2}{\eta_0} \ln \frac{b}{a}.$$

As might be expected, this result shows that power capacity can be increased by using a larger coaxial cable (larger a, b with fixed b/a for the same characteristic impedance). However, propagation of higher order modes limits the maximum operating frequency for a given cable size. Thus, there is an upper limit on the power capacity of a coaxial line for a given maximum operating frequency, f_{\max} , which can be shown to be given by

$$P_{\max} = \frac{0.025}{\eta_0} \left(\frac{c E_d}{f_{\max}} \right)^2 = 5.8 \times 10^{12} \left(\frac{E_d}{f_{\max}} \right)^2.$$

As an example, at 10 GHz the maximum peak power capacity of any coaxial line with no higher order modes is about 520 kW.

In an air-filled rectangular waveguide the electric field varies as $E_y = E_o \sin(\pi x/a)$, which has a maximum value of E_o at $x = a/2$ (the middle of the guide). Thus the maximum power capacity before breakdown is

$$P_{\max} = \frac{ab E_o^2}{4Z_w} = \frac{ab E_d^2}{4Z_w},$$

which shows that power capacity increases with guide size. For most standard waveguides, $b \simeq 2a$. To avoid propagation of the TE_{20} mode we must have $a < c/f_{\max}$, where f_{\max} is the

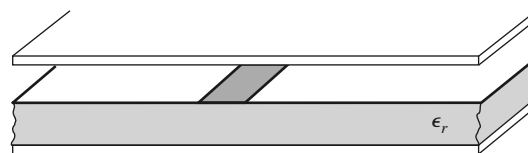


FIGURE 3.35 Covered microstrip line.

maximum operating frequency. Then the maximum power capacity of the guide can be shown to be

$$P_{\max} = \frac{0.11}{\eta_0} \left(\frac{c E_d}{f_{\max}} \right)^2 = 2.6 \times 10^{13} \left(\frac{E_d}{f_{\max}} \right)^2.$$

As an example, at 10 GHz the maximum peak power capacity of a rectangular waveguide operating in the TE_{10} mode is about 2300 kW, which is considerably higher than the power capacity of a coaxial cable at the same frequency.

Because arcing and voltage breakdown are high-speed transient effects, these voltage and power limits are peak values; average power capacity is lower. In addition, it is good engineering practice to provide a safety factor of at least two, so the maximum powers that can be safely transmitted should be limited to about half of the above values. If there are reflections on the line or guide, the power capacity is further reduced. In the worst case, a reflection coefficient magnitude of unity will double the maximum voltage on the line, so the power capacity will be reduced by a factor of four.

The power capacity of a line can be increased by pressurizing the line with air or an inert gas or by using a dielectric. The dielectric strength (E_d) of most dielectric materials is greater than that of air, but the power capacity may be further limited by the heating of the dielectric due to ohmic loss.

Reference: P. A. Rizzi, *Microwave Engineering—Passive Circuits*, Prentice-Hall, Englewood Cliffs, N.J., 1988.

REFERENCES

- [1] O. Heaviside, *Electromagnetic Theory*, Vol. 1, 1893. Reprinted by Dover, New York, 1950.
- [2] Lord Rayleigh, "On the Passage of Electric Waves through Tubes," *Philosophical Magazine*, vol. 43, pp. 125–132, 1897. Reprinted in *Collected Papers*, Cambridge University Press, Cambridge, 1903.
- [3] K. S. Packard, "The Origin of Waveguides: A Case of Multiple Rediscovery," *IEEE Transactions on Microwave Theory and Techniques*, vol. MTT-32, pp. 961–969, September 1984.
- [4] R. M. Barrett, "Microwave Printed Circuits—An Historical Perspective," *IEEE Transactions on Microwave Theory and Techniques*, vol. MTT-32, pp. 983–990, September 1984.
- [5] D. D. Grieg and H. F. Englemann, "Microstrip—A New Transmission Technique for the Kilomegacycle Range," *Proceedings of the IRE*, vol. 40, pp. 1644–1650, December 1952.
- [6] H. Howe, Jr., *Stripline Circuit Design*, Artech House, Dedham, Mass., 1974.
- [7] I. J. Bahl and R. Garg, "A Designer's Guide to Stripline Circuits," *Microwaves*, January 1978, pp. 90–96.
- [8] I. J. Bahl and D. K. Trivedi, "A Designer's Guide to Microstrip Line," *Microwaves*, May 1977, pp. 174–182.
- [9] K. C. Gupta, R. Garg, and I. J. Bahl, *Microstrip Lines and Slotlines*, Artech House, Dedham, Mass., 1979.

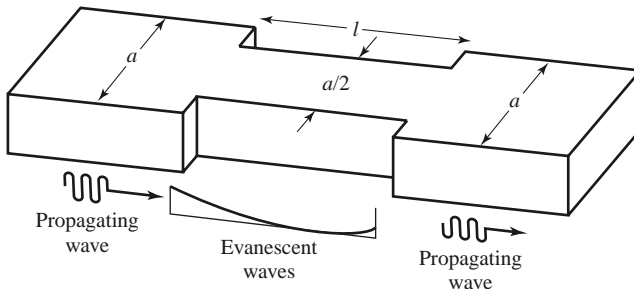
PROBLEMS

- 3.1** Devise at least two variations of the basic coaxial transmission line geometry of Section 3.5, and discuss the advantages and disadvantages of your proposed lines in terms of size, loss, cost, higher order modes, dispersion, or other considerations. Repeat this exercise for the microstrip line geometry of Section 3.8.
- 3.2** Derive equations (3.5a)–(3.5d) from equations (3.3) and (3.4).
- 3.3** Calculate the attenuation due to conductor loss for the TE_n mode of a parallel plate waveguide.
- 3.4** Consider a section of air-filled K-band waveguide. From the dimensions given in Appendix I, determine the cutoff frequencies of the first two propagating modes. From the recommended operating range given in Appendix I for this guide, determine the percentage reduction in bandwidth

that this operating range represents, relative to the theoretical bandwidth for a single propagating mode.

3.5 A 10 cm length of a K-band copper waveguide is filled with a dielectric material with $\epsilon_r = 2.55$ and $\tan \delta = 0.0015$. If the operating frequency is 15 GHz, find the total loss through the guide and the phase delay from the input to the output of the guide.

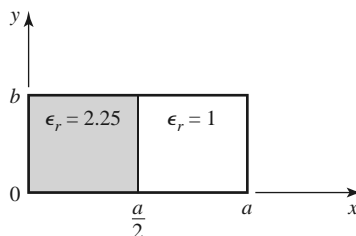
3.6 An attenuator can be made using a section of waveguide operating below cutoff, as shown in the accompanying figure. If $a = 2.286$ cm and the operating frequency is 12 GHz, determine the required length of the below-cutoff section of waveguide to achieve an attenuation of 100 dB between the input and output guides. Ignore the effect of reflections at the step discontinuities.



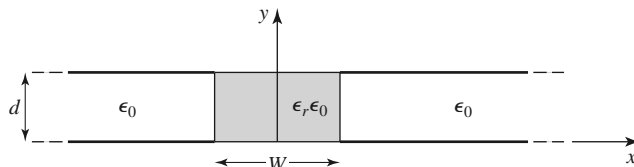
3.7 Find expressions for the electric surface current density on the walls of a rectangular waveguide for a TE_{10} mode. Why can a narrow slot be cut along the centerline of the broad wall of a rectangular waveguide without perturbing the operation of the guide? (Such a slot is often used in a slotted line for a probe to sample the standing wave field inside the guide.)

3.8 Derive the expression for the attenuation of the TM_{mn} mode of a rectangular waveguide due to imperfectly conducting walls.

3.9 For the partially loaded rectangular waveguide shown in the accompanying figure, solve (3.109) with $\beta = 0$ to find the cutoff frequency of the TE_{10} mode. Assume $a = 2.286$ cm, $t = a/2$, and $\epsilon_r = 2.25$.



3.10 Consider the partially filled parallel plate waveguide shown in the accompanying figure. Derive the solution (fields and cutoff frequency) for the lowest order TE mode of this structure. Assume the metal plates are infinitely wide. Can a TEM wave propagate on this structure?



3.11 Derive equations (3.110a)–(3.110d) for the transverse field components in terms of longitudinal fields, in cylindrical coordinates.

3.12 Derive the expression for the attenuation of the TM_{nm} mode in a circular waveguide with finite conductivity.

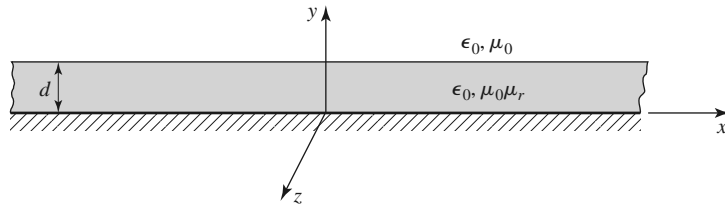
3.13 A circular copper waveguide has a radius of 0.4 cm and is filled with a dielectric material having $\epsilon_r = 1.5$ and $\tan \delta = 0.0002$. Identify the first four propagating modes and their cutoff frequencies. For the dominant mode, calculate the total attenuation at 20 GHz.

3.14 Derive the \bar{E} and \bar{H} fields of a coaxial line from the expression for the potential given in (3.153). Also find expressions for the voltage and current on the line and the characteristic impedance.

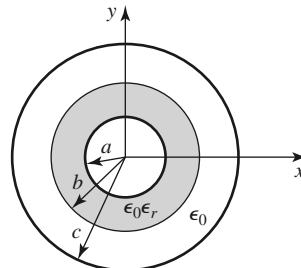
3.15 Derive a transcendental equation for the cutoff frequency of the TM modes of a coaxial waveguide. Using tables, obtain an approximate value of $k_c a$ for the TM_{01} mode if $b/a = 2$.

3.16 Derive an expression for the attenuation of a TE surface wave on a grounded dielectric substrate when the ground plane has finite conductivity.

3.17 Consider the grounded magnetic substrate shown in the accompanying figure. Derive a solution for the TM surface waves that can propagate on this structure.



3.18 Consider the partially filled coaxial line shown in the accompanying figure. Can a TEM wave propagate on this line? Derive the solution for the TM_{0m} (no azimuthal variation) modes of this geometry.



3.19 A copper stripline transmission line is to be designed for a 100Ω characteristic impedance. The ground plane separation is 1.02 mm and the dielectric constant is 2.20, with $\tan \delta = 0.001$. At 5 GHz, find the guide wavelength on the line and the total attenuation.

3.20 A copper microstrip transmission line is to be designed for a 100Ω characteristic impedance. The substrate is 0.51 mm thick, with $\epsilon_r = 2.20$ and $\tan \delta = 0.001$. At 5 GHz, find the guide wavelength on the line and the total attenuation. Compare these results with those for the similar stripline case of the preceding problem.

3.21 A 100Ω microstrip line is printed on a substrate of thickness 0.0762 cm with a dielectric constant of 2.2. Ignoring losses and fringing fields, find the shortest length of this line that appears at its input as a capacitor of 5 pF at 2.5 GHz. Repeat for an inductance of 5 nH. Using a microwave CAD package with a physical model for the microstrip line, compute the actual input impedance seen when losses are included (assume copper conductors and $\tan \delta = 0.001$).

3.22 A microwave antenna feed network operating at 5 GHz requires a 50Ω printed transmission line that is 16λ long. Possible choices are (1) copper microstrip, with $d = 0.16$ cm, $\epsilon_r = 2.20$, and $\tan \delta = 0.001$, or (2) copper stripline, with $b = 0.32$ cm, $\epsilon_r = 2.20$, $t = 0.01$ mm, and $\tan \delta = 0.001$. Which line should be used if attenuation is to be minimized?

3.23 Consider the TE modes of an arbitrary uniform waveguiding structure in which the transverse fields are related to H_z as in (3.19). If H_z is of the form $H_z(x, y, z) = h_z(x, y)e^{-j\beta z}$, where $h_z(x, y)$ is a real function, compute the Poynting vector and show that real power flow occurs only in the z direction. Assume that β is real, corresponding to a propagating mode.

3.24 A piece of rectangular waveguide is air filled for $z < 0$ and dielectric filled for $z > 0$. Assume that both regions can support only the dominant TE_{10} mode and that a TE_{10} mode is incident on the interface from $z < 0$. Using a field analysis, write general expressions for the transverse field components of the incident, reflected, and transmitted waves in the two regions and enforce the boundary conditions at the dielectric interface to find the reflection and transmission coefficients. Compare these results to those obtained with an impedance approach, using Z_{TE} for each region.

3.25 Use the transverse resonance technique to derive a transcendental equation for the propagation constant of the TM modes of a rectangular waveguide that is air filled for $0 < x < d$ and dielectric filled for $d < x < a$.

3.26 Apply the transverse resonance technique to find the propagation constants for the TE surface waves that can be supported by the structure of Problem 3.17.

3.27 An X-band waveguide filled with Rexolite is operating at 9.0 GHz. Calculate the speed of light in this material and the phase and group velocities in the waveguide.

3.28 As discussed in the Point of Interest on the power-handling capacity of transmission lines, the maximum power capacity of a coaxial line is limited by voltage breakdown and is given by

$$P_{\max} = \frac{\pi a^2 E_d^2}{\eta_0} \ln \frac{b}{a},$$

where E_d is the field strength at breakdown. Find the value of b/a that maximizes the maximum power capacity and show that the corresponding characteristic impedance is about 30Ω .

3.29 A microstrip circuit is fabricated on an alumina substrate having a dielectric constant of 9.9, a thickness of 2.0 mm, and a 50Ω linewidth of 1.93 mm. Find the threshold frequencies of the four higher order modes discussed in Section 3.8, and recommend the maximum operating frequency for this microstrip circuit.